Regulation of Apoptosis in Human Cancer Cells

by

S. Julie-Ann Lloyd

S. B. Chemistry (2003)
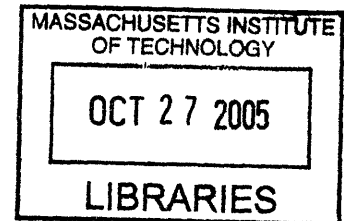
Massachusetts Institute of Technology

Submitted to the Biological Engineering Division in Partial
Fulfilment of the Requirements for the Degree of Master of
Science in Biological Engineering

at the

Massachusetts Institute of Technology

June 2005

Signature of Author: _____
Division of Biological Engineering
6th May 2005

Certified by: _____

Steven Robert Tannenbaum, Ph.D.
Underwood Prescott Professor of Toxicology
Professor of Chemistry
Thesis Supervisor

Accepted by: _____

Ram Sasisekharan, Ph.D.
Professor of Biological Engineering
Chair, Biological Engineering Division Graduate Committee

Regulation of Apoptosis in Human Cancer Cells

by

S. Julie-Ann Lloyd

Submitted to the Biological Engineering Division on
6th May 2005 in Partial Fulfilment of the Requirements for
the Degree of Master of Science in Biological Engineering

ABSTRACT

Nitric oxide is postulated to protect cancer cells from the death-inducing effects of tumour necrosis factor alpha by S-nitrosating the active site cysteines, inhibiting cleavage of caspase-9. We aimed to test this hypothesis and to determine its validity across cancer cell types. In addition, we hoped to explain the involvement of certain kinases in nitric oxide-induced apoptosis. The experimental setup involved stimulating human colorectal cancer cells, HT-29 and HCT-116, and human prostate cancer cells, LNCaP, with cytokines in order to induce cell death. Then, we observed the effects of NO inhibitors, kinase inhibitors, and activation of Akt, a kinase up-stream of the caspase cascade, following transfection of a DNA sequence that was proven to protect cells against apoptosis induction. In our series of experiments, inhibition of the nitric oxide synthases removes nitric oxide protection from apoptosis, but inhibition of only the inducible synthase has opposite effects with prostate and colon cancer cells that are considered insignificant, and its effects on the two types of colon cancer cells are in discord. Transformation and transfection of ARK5 into the colorectal cancer cell line, HT-29 did not prove beneficial. Similarly, glucosamine showed no clear pattern of reducing apoptosis in the cells. Therefore, we propose further exploration of the inhibition of constitutive nitric oxide synthases as a potential therapy.

Thesis Supervisor: Steven R. Tannenbaum
Title: Underwood Prescott Professor of Toxicology and Professor of Chemistry

TABLE OF CONTENTS

Regulation of Apoptosis in Human Cancer Cells.1

LIST OF TABLES AND FIGURES

4

ACKNOWLEDGMENTS

1. INTRODUCTION

Diseases [in human beings] are progressively more resistant to currently available drugs. How best to neutralise this challenge, in light of the sharp rise in life expectancy amongst the U.S. population, and the rate of technological change are two of the factors that have significant impact on scientific research for cures to diseases, such as cancers.

A 2003 experimental project executed by a team in the Tannenbaum laboratory [and on which I was a partner], established that glucosamine modulates the production of inflammatory molecules through the mitogen-activated protein kinase (MAPK) pathway. Nitric oxide (NO) had been shown separately to protect HT-29 colon cancer cells from apoptosis through S-nitrosation of the active site cysteine. The implication of these findings formed the rationale for studying the consequence of NO on cancer cells to determine whether the observed effects were universal or at least a cancer-specific phenomenon. Additional investigation will also be conducted into glucosamine as an instrumental factor in apoptosis that is induced in cancer cells by cytokines (or drugs).

Nitric oxide has both physiological benefits and harmful effects on the body. It maintains physiological homeostasis, regulates the cardiovascular system and promotes cellular adhesion for tissue formation. As an antioxidant, NO protects the body against the toxic effects of tumour necrosis factor and apoptosis (the natural, programmed cell death), due to changes in the health and condition of normally functioning cells (25). The practical application of NO to diseases, such as diabetes, atherosclerosis, myocardial infarction and cancer is wide-ranging. With additional research, NO inhibition has the potential of warding off cancer cells' evasion of cell death.

1.1 Objectives of the Study

The underlying study has a four-prong approach. Its expected results will clarify whether and, if so, how cancer cells bypass the mechanism of apoptosis. In addition, we expect that our findings will provide a means by

which to target and, therefore, realise controlled cell death. Particulars of this study's aims have been delineated below, as follows:

- Investigate the hypotheses, NO protects cancer cells against apoptosis, and inhibitors of nitric oxide synthase (NOS) increase cell susceptibility to apoptosis;
- Determine whether or not the underlying study results are universal to all human cancer cell types.
- Examine the effects of glucosamine, an inhibitor of externally regulated kinase (ERK) on apoptosis involving the MAPK pathway.
- Utilise alternative sequences of biochemical reactions, such as the Akt pathway, to exploit caspase activation.

Cancer is the principal cause of death among the U.S. adult population (20). Tumours of the lung and bronchus (29% deaths), breast (15% deaths), prostate (10% deaths), and colon and rectum (10% deaths) account for the highest death rates in both genders. Cancer incidence is a measure of the number of *new* cases in a given year per 100,000 people (for gender-specific cancers; same-gender patients comprise the denominator).

The rate of cancer incidence became stable around the mid-2000s, due to new advances in research and lifestyles changes in the U.S. population. Early detection through screening has also had a favourable outcome in cancer treatments, with effective tests available to screen for a number of cancers (notably, breast and cervical types). In contrast to these positive developments, the screening rate for colorectal cancer remains unacceptably low.

The regular post-surgery therapy for cancer is chemotherapy, which is a combination of toxins that attack all actively reproducing cells, especially those in the M and S phases of the cell cycle. The treatment unsystematically targets cancerous and non-cancerous cells, alike, with hair loss during treatments as its most discernable side effect. Ideally, this form of therapy should be selective, affecting only the tumour cells. Because cancer cells sometimes develop mechanisms to bypass the ordinary mechanisms of death, directed cell attack currently pose a sizeable challenge.

2. RATIONALE AND SIGNIFICANCE

The current canon holds that animal cells derive specific survival signals from other cells. Signals of this type activate or suppress suicide programs and, when transformed, the unwanted cells die and are phagocytosed. The tenet also postulates that non-pathological cell death, also known as apoptosis, occurs normally at the developmental stage and is useful in determining cell number and tissue size. Apoptosis is apparent, for instance, in the formation of fingers from selective death of the tissue that is initially present between digits.

Apoptosis morphology consists of nuclear condensation, cytoplasmic shrinkage, membrane blebbing and blister formation. Note that organelles (other than the endoplasmic reticula) showed no swelling or changes in functioning, nor was there any leakage of call contents; hence, inflammation did not occur (32). Instead, the phosphatidylserine residues gather about the outer surface of the plasma membrane, activating proteases. The procedure requires energy for mRNA and protein synthesis (16).

Inherent in each cell is a vim that is analogous to a killing machine. Typically, this force is dormant, but will rapidly go into killing mode when death is signalled from its inhibition and, correspondingly, the cell is induced to die (32). This induced cell death depends upon factors, such as the stage of the cell cycle, the strength of competing signals and the relative expression of pro-apoptotic and anti-apoptotic proteins. Given the occurrence of a blocked apoptosis pathway, for instance, the cell might die through autophagy or other unspecified pathway.

Occasionally, cells develop means of bypassing cell death by apoptosis or otherwise. This phenomenon leads to uncontrollable and, in some cases, cancerous, cell growth. To inhibit the onset of cancer and develop better treatments, an understanding of the physiology of the system, and the cause and progression of its abnormality is useful.

2.1 Apoptosis Induction by Surface Receptors

Apoptosis can start from ligation of death receptors in the tumour necrosis factor (TNF-R) family (namely, CD95/Fas/Apo-1/TNFR1/TRAIL-R), by

their respective cytokines. As has been illustrated in Figure 1, ligands binding to plasma membrane receptors recruit Fas-associated death domain protein (FADD) and TNFR1-associated death domain protein (TRADD), both of which cause down-stream initiation of proteolytic enzymes (25), tagged caspases or cysteine-requiring aspartate specific proteases. These reactions occur in caspase-dependent apoptosis. It is also plausible that apoptosis can be caspase-independent, with associated stimuli comprising granzyme B from virally infected cytotoxic T-cells, UV-light, X-rays and chemotherapeutic drugs, and deprivation of growth factors and interleukin-2 (IL-2). However, the majority of apoptotic reactions involve caspases that can be regulated.

2.2   The Caspase Cascade

Caspases are cysteine proteases that disable critical homeostatic and repair processes, by cleaving after the aspartic acid residue. An examination of the recognised active site indicates QACXG, where, the variable, X, is any residue. As the apoptotic bodies become engulfed, proteases cause the systematic and orderly disassembly of the dying cell, through the degradation of proteins that are required for cytoskeletal regulation. In a proteolytic cascade involving autocatalysis, caspases de-activate inhibitors and cleave and trigger other caspases into long and short domains, which associate to form heterodimers. They then associate and act as catalytically active tetramers with two functionally independent, catalytic sites (4) to initiate and sustain either receptor-linked apoptosis or cell death that is linked to mitochondrial metabolism.

All caspases are not essential in the process of cell death. Caspases consist of subfamilies, and their division reflects structural similarity, sequence similarity and preference for substrate. Alternative splicing throughout activation forms different variations on the original zymogen. By implication, the apoptotic pathway typifies some combination of caspases but, ultimately, the overall scheme entails a two-tier activation of specific members of the caspase class: the commitment phase and the execution phase. Caspases 8, 9 and 10 situate at the upper end of the cascade, and down-stream are caspases 3, 6, and 7, whose cellular substrates include poly-ADP ribose polymerase

(PARP), lamins and histones. Each of these has a DXXD motif (Figure 2) similar to that described in PARP (4). In particular, caspase-3 cleaves PARP at DEVDG, freeing up the PARP substrate, adenosine triphosphate (ATP) for the energy-dependent apoptosis reactions. Furthermore, caspase-3 (as well as granzyme B) activates down-stream caspase-9, whose over-expression triggers apoptotic events and cause further cleavage at QACXG active sites, where the variable, X, is glycine.

In later apoptotic events, proteins localised in the mitochondria -- second mitochondria-derived activator of caspases/direct IAP binding protein with low PI (SMAC/DIABLO), arylhydrocarbon receptor–interacting protein (AIP) and cytochrome c -- are released. SMAC/Diablo binds anti-apoptotic IAP proteins, suppressing their inhibitory activity and promoting caspase activation (7,56). When cyotchrome c is present in the cytoplasm, Apaf-1 oligomerises and combines with ATP and procaspse-9, as revealed in Figure 1, to form the apoptosome (25).

The action of caspases is irreversible; therefore, caspase regulation occurs through control of both activity and availability of the substrate. Naturally occurring CrmA and Bcl-2, p35 and peptide inhibitors, and reversible inhibitors (such as aldehydes, ketones and nitriles), can counteract caspase activity (4). Bcl-2 proteins' chief role is detection of cellular stress in the cytoplasm they routinely reposition by rising to the mitochondrial surface. There, pro-apoptotic and anti-apoptotic bcl-2 proteins interact to form pores in the mitochondria. The next course of action is a release of cytochrome c, which causes formation of the apoptosome with caspase-9 and activates the caspase cascade. As a consequence of this process, the majority of pathological treatments have focused on the direct activation of caspases, control of their selectivity and the exploitation of oncogenic transformation.

2.3 Nitric Oxide Production

A stable, free radical, NO is a neutral, lipophilic molecule with a weak chemical reactivity with thiols at neutral pH. Previous studies indicate that the radical is formed from a two-step oxidation of L-arginine into citrulline from the terminal guanidine nitrogen of L-arginine (33). Large phagocytic cells of the

reticuloendothelial system, called macrophages, produce the diatomic molecule in a reaction (shown in Equation 1) that is mediated by each of three types of nitric oxide synthase. (A fourth isoform, mtNOS has been recently discovered in the mitochondria.)

$$\text{L-Arginine} + O_2 \longrightarrow \text{Citrulline} + NO\bullet \qquad \textbf{(Equation 1)}$$

The NOS isozymes exist as homodimers, with molecular weights ranging between 130 and 160 kDa, and require co-factors, nicotinamide adenine dinucleotide phosphate (NADPH), flavin dinucleotide (FAD), flavin mononucleotide (FMN), tetrahydrobiopterin, haem and BH_4. Additionally, NOS activity is a function of their localization inside the cells; their regulation is complex and cell-specific (25). The constitutive, forms, neuronal NOS (nNOS) and endothelial NOS (eNOS), are modulated mostly at the post-translational level by a multitude of different stimuli in diverse cell types through calcium/calmodulin activation. Over prolonged periods of time, inducible NOS (iNOS) produces high (micromolar) and sustainable levels of NO under the transcriptional control of the pro-inflammatory agents. Specifically, iNOS is up-regulated due to a synergism of various stimuli, including tumour necrosis factor (TNF), interferons (IFN) and bacterial lipopolysaccharide (LPS), nuclear factor kappa b (NFκB), activator protein 1 (AP-1), cAMP and other second messengers (25). Its down-regulation occurs in response to transforming growth factor (TGF), heat shock protein (Hsp), the tumour suppressor gene, p53, and, in a negative feedback loop, NO. There is no correlation between NO activity and iNOS mRNA expression, suggesting post-transcriptional regulation. iNOS over-expression during chronic inflammation leads to mutagenesis and cell death (42).

Nitric oxide is highly reactive and diffusive. As a charged, chemically active molecular fragment, deficient in electrons, it reacts directly with other molecules especially haem-containing compounds, or indirectly through the formation of reactive nitrogen species (RNOS): nitrogen trioxide (N_2O_3), transferred as the nitrosonium cation (NO+) to an active site thiol of cysteine in a protein; nitroxyl (HNO) and peroxynitrite (ONOO-), which oxidise thiol-containing proteins (9). The target amino acid must be in its reduced state for

the reaction to progress, and the type of reaction will depend on the redox potential of the cell (30,34,36). The biological activity of NO hinges on its unpaired electron and, as such, it also reacts with electron acceptors (notably, oxygen), transition metal ions and superoxide radicals, which will continue in other S-nitrosation reactions (24).

2.4   Apoptotic Effects of Nitric Oxide

Nitric oxide is a pleiotrophic regulator that is important in a diversity of responses (namely, vasodilation, neurotransmission and macrophage-mediated immunity). Diseases, such as vascular dysfuntions, cerebral infarction and diabetes mellitus are associated with faulty production of NO. The effects of NO on the body are somewhat contradictory, and conflicting reports from the scientific community have otherwise obscured its true impact of NO on cells. Many variables play into NO reactivity; its source, concentration and form within the cell, cell-type and the presence of antioxidants (25) can affect whether NO is beneficial or harmful. Specific to this discussion, NO can be both pro-apoptotic and anti-apoptotic, depending on the cell type and redox status, the concentration of NO and the presence or absence of certain co-factors.

Amongst the relevant variables or factors are Bcl-2 proteins; antioxidants (namely, metals conjugated to superoxide dismutase); repeated exposure to cytokines; iron, which is protective to the cell; the presence and concentration of arginase, which competes with iNOS for the arginine substrate; prostaglandins, such as cyclo-oxygenase 2 (COX-2), that inhibit apoptosis; and glucose, which, at high levels, produce ROS and NO that lead to apoptosis, increase the ATP level to prevent energy depletion, and determines the type of cell death (necrosis versus apoptosis).

Nitric oxide is involved in both ligand-dependent and ligand-independent apoptosis, inducing apoptosis through the action of reactive nitrogen species (RNOS), formed by reaction with NO and ROS. These RNOS react directly with DNA. Peroxynitrite, a S-nitrosating species, oxidises DNA, causing strand breaks that can lead to further damage by up-regulating p53 and activating PARP. Peroxynitrite also specifically targets thiols (inhibiting DNA repair and

12

synthesis) degrades proteins and induces lipid peroxidation (2). Nitrogen trioxide (N_2O_3) also leads to nitrosation of amines and the formation of other mutagens that damage DNA.
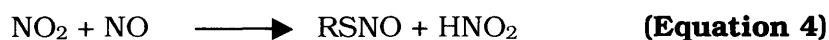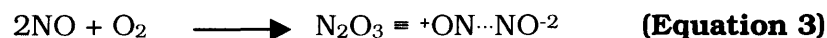
Another primary NO-dependent pathway by which to trigger apoptosis is up-regulation of p53. This increases the amounts of pro-apoptotic Bax present relative to anti-apoptotic Bcl-XL; thereby, activating caspases (Figure 3). A change in the bcl-2 protein ratio plus the presence of second messengers, calcium, ceramide derivatives, nitric oxide, and reactive oxygen species, and pro-apoptotic Bax, Bid, Bak and caspases can alter the mitochondrial membrane potential. Note that, at low NO concentrations, such a change is reversible and, at high NO concentrations, it is irreversible (24).

These alterations are modulated through the permeability transition pore (PTP) of the mitochondria. However, cancerous cells produce proteins that bind to and inactivate p53. They also produce proteins similar to bcl-2 or increase the production of bcl-2, thereby reducing the likelihood of apoptosis. The apoptosis promoter, p53, also suppresses iNOS production; hence, p53 mutation, functional loss, activation and inactivation of apoptotic proteins are all linked to NO resistance (42). Experiments in macrophages have shown that apoptosis occurs via the JNK/SAPK pathway and that over-experession of protein kinase C (PKC) protects these cells against NO-induced apoptosis. Further, p38 MAPK has been implicated in apoptosis in neuronal and haematopoietic cells (21).

Additional mechanisms of reducing the frequency of apoptosis induction include the binding to the haem moiety of guanylyl cyclase and activation of cGMP, signalling and suppressing of caspases activity, increasing the expression of anti-apoptotic proteins, and inhibiting the proteasome. These effects indicate that NO-induced apoptosis occurs through the 20S and 26S subunits. Conversely, NO inhibits apoptosis by moderating cyclic nucleotides, specifically cGMP and cAMP by mechanisms similar to those cited above, but devoid of any overlap in cell types. Current literature does not offer any explanation of this discrepancy.

At low concentrations, NO has direct cytostatic effects on the body. In combination with metals in prosthetic groups, it reacts to form stable metal ion

13

complexes, which inhibits the activities of the related enzymes and alter the synthesis or metabolism of many molecules, such as lipids (56). It reacts with other free radicals to suppress DNA synthesis and increase sensitivity to radiation. NO also causes cells to become more susceptible to the cytotoxins, preventing cell growth and division and promoting damage to healthy, noncancerous tissue. These indirect effects stem from oxidation (the removal of one or more electrons from the substrate), nitration (the addition of NO_2^+ to an aromatic group) or nitrosation (the addition of NO^+ to an amine, thiol or hydroxy aromatic group). In this case, S-nitrosation of the active site cysteines in caspases protects the cells from apoptosis. The reaction usually proceeds at only one thiol within a given protein, though there are many such sites (24).

$$^+ON\cdots NO^{-2} + RSH \longrightarrow 2\ NO_2 \qquad \textbf{(Equation 2)}$$

$$2NO + O_2 \longrightarrow N_2O_3 \equiv\ ^+ON\cdots NO^{-2} \qquad \textbf{(Equation 3)}$$

$$NO_2 + NO \longrightarrow RSNO + HNO_2 \qquad \textbf{(Equation 4)}$$

Where, R is the substrate to be nitrosated, forming the generic structure (RSNO) of S-nitrosothiols. This reaction scheme, depicted in Equations 2 through 4, results in a reversible, post-translational modification of a protein structure that affects its ability to repair DNA, transduce signals, and activate or inhibit enzymes in cellular processes, especially apoptosis (24), ubiquitous regulatory mechanisms and other redox-sensitive signalling pathways, including the mitogen-activated protein kinase (MAPK) pathway (40). The rate-limiting step, under physiological conditions, is the production of nitrogen dioxide (NO_2) from nanomolar concentrations of nitrogen monoxide (NO) and micromolar concentrations of oxygen (13). However, the preferred targets are cysteines in hydrophobic compartments, such as biological membranes, because the hydrophobic phase has large local concentrations of NO_2 and NO. Hence, its expected effect is an increase in the reaction rate between these two compounds. In addition, SNO bioactivities are typically stereoselective (13); NO targets cysteine thiols with distinctive temporal resolution and three-dimensional protein configuration (17).

Once S-nitrosation has occurred, Bid and Bcl-2 cleavage is inhibited and, consequently, cytochrome c release from the mitochondria is avoided. The

14

formation of nitrogen oxide is further favoured by co-localisation of NO sources and targets with subcellular precincts, based on some specific protein-protein interactions with NO synthases (17), and catalysed by electron acceptors, such as nicotinamide adenine dinucleotide (NAD+), iron-nitrosyls and specific proteins with consensus motifs.

Formation of S-nitrosothiols results from activation of any of the three nitric oxide synthases, reaction between NOS-derived NO-/NO/NO+ with target protein motifs and metalloprotein-catalysed reactions. To prevent their reductive or transnitrosative degradation, S-nitrosothiols can be sequestered in membranes, lipophilic protein folds, in vesicles and in interstitial spaces (14). For instance, caspases are usually sequestered in an inactive state to the mitochondrial membrane space and, during apoptosis, the caspases are released into the cytoplasm where they can be denitrosated and activated. In contrast to this procedure, S-nitrosothiols degradation employs a number of enzyme systems, such as glutathione-dependent formaldehyde dehydrogenase (GDFDH) and the thioredoxin/thioredexin reductase system (14). They decompose, presumably by homolytic cleavage of the S-N bond, to give nitric oxide (NO•) and the corresponding disulphide or thiyl radical (44). The presence of transition metal ions and photolytic conditions promote the reaction, but the S-N bond is otherwise stable, especially in the presence of transition metal ion chelators in the dark.

At physiological NO concentrations, NO inhibits PTP opening and this action prevents the release of cytochrome c into the cytoplasm. NO directly interacts with p53, and this exchange not only alters its activity, but also inhibits apoptosis (42).

2.5   Inhibitors of Nitric Oxide Synthases

Overproduction of NO plays a role in many disorders. It facilitates direct NO interaction, for instance, and contributes to arthritis, septic shock, diabetes and various neurodegenerative diseases. This over-stimulation is usually attributable to up-regulation of iNOS in response to proinflammatory cytokines.

Control of NO production would regulate the amount of highly toxic and reactive products, specifically the previously mentioned peroxinitrite. Animal

studies have shown that controlling NO production can be therapeutic and could further elucidate biological mechanisms and functions of NO. However, an ideal solution would involve the use of drugs that target only the inducible isoform of NOS without affecting the levels of eNOS, which is crucial to vasoregulation in the endothelium, or nNOS. In fact, long-term inhibition of the constitutive forms of NOS leads to pathological disorders, such as hypertension and organ injury (5). Alternatively, the immune system response could be altered to regulate the relative production of iNOS (6).

Already in common use is an indiscriminate inhibitor of NOS, known as N-monomethyl-L-arginine (L-NMA), that inhibits proteoglycan synthesis by IL-1β and increases the concentration of TGF-β (47). However, this inhibitor is, at best, 30-fold more effective against iNOS than eNOS. The iNOS-specific inhibitors, aminoguanidine and N-(3-(Aminomethyl)benzyl)acetamidine (1400W), show anti-inflammatory effects by selectively inhibiting iNOS (11,12,45,46). In particular, Garvey, et al, (1997) illustrated that, in vascular tissue and in a time-dependent manner, 1400w inhibited iNOS 200- to 5000-fold more effectively than eNOS and nNOS without toxicity. The explanation lay in the structure of 1400W, whose primary sequence includes amidine, a structural analogue of guanidine and either competes with guanidine for the active site or allosterically inhibit iNOS. The Garvey experimentation team concluded that 1400W worked as an irreversible inhibitor or a slowly reversible inhibitor. However, our study will investigate changes over a short period during which 1400W has ample time to affect the cells' apoptotic profile.

2.6   Glucosamine Effect on Inflammation

Inflammation occurs as a localised protective response to injury that is characterised by an elevation in the levels of NO. Glucosamine (or 2-amino-2-deoxy-D-glucose) is a natural metabolite of glutamine and fructose-6-phosphate used to treat inflammation as a symptom of osteoarthritis (OA) (50). In OA, osteoclast activity is elevated, causing an imbalance between the synthesis and degradation of cartilage and, ultimately, leading to loss of cartilage (19).

Glucosamine has been shown to be abundant in many complex polysaccharides, connective tissue and cartilage, where it helps to preserve

their strength, flexibility, and elasticity. In addition to its structural role in the extracellular matrix, glucosamine may inhibit the activation of inflammatory cell types involved in the OA disease process, including chondrocytes and macrophages (35). This is an area of opportunity for added study since the mechanisms of glucosamine efficacy are still unknown. Hypotheses might include the signal transduction pathway between the binding of LPS and IFN-γ to their respective membrane receptors and the induction of inflammatory genes.

Glucosamine is believed to increase both the activity of agrecanase (10) and the synthesis of structural proteoglycans in joint cartilage by mediating the effects of a cytokine, IL-1β (15). Secretion of IL-1β by activated macrophages occurs in response to antigens and results in the inflammation of joints. The cytokine initiates a series of events, including the inhibition of glycosaminoglycan (GAG) biosynthesis and results in the prevention of proteoglycan synthesis, which could ultimately lead to cartilage deterioration. The latter also relates to an increased production of nitric oxide and inducible nitric oxide synthase. Glucosamine has been proven to inhibit this increase in the synthesis of inducible iNOS and NO (61). Research has confirmed the formation of glucosamine from its glutamine precursors indirectly inhibits the pentose cycle pathway, thereby reducing the availability of the iNOS cofactor, nicotinamide dinucleotide phosphate (NADPH) (61).

These inflammatory effects can be replicated in macrophage cell cultures treated with LPS and IFN-γ. There are defined pathways between receptor binding of LPS and iNOS expression. LPS activates the interferon inducible gene, interferon response factor one (IRF-1) (39), thereby increasing the transcription of the LPS binding protein, CD48, and inducing the iNOS gene. The binding of IFN-γ to its receptor increases TNF-α production through the activation of the JAK-STAT pathway (59). LPS also activates the toll like receptor, which transmits via MyD88, IRAK and TRAF6 to activate NFκB as well as several members of the mitogen-activated protein kinase (MAPK) family (62). MAPKs are known to activate a number of transcription factors, including AP-1, ATF-2, CREB and certain members of the Ets family (52). These MAPK responsive transcription factors promote the induction of inflammatory genes such as iNOS, members of the matrix metalloproteinase family and TNFα (3,37).

17

2.7 Other Signalling Pathways

The association of MAPK in TNF-α-induced apoptosis impelled additional investigation into alternative signalling pathways, including the Akt pathway, which is up-stream of caspase activation [and apoptosis] and purported to be under the effects of TNF-α (48). Embedded in the Akt pathway is adenosine monophosphate-activated protein kinases (AMPK), known to play a key, signalling role in response to nutrients throughout evolution.

ARK5 is a 661 amino acid protein, with a molecular weight of 74 kiloDaltons. It shares homology with other members of the AMPK family, specifically 47%, 45.8%, 42.4% and 55% with AMPK-α1, AMPK-α2, MELK and SNARK, respectively (49). Thus, ARK is a serine/threonine protein kinase that is activated by AMP under conditions of stress, such as reduced ATP concentrations and, along with other members of the AMPK family, is necessary to maintain energy equilibrium within the cells. The amino acid sequence of ARK5 revealed a conserved region near the C-terminal that serves as the active site for Akt phosphorylation; that is, Akt phosphorylates ARK5 at Ser[600]. ARK5 mRNA is expressed in the heart, brain, skeletal muscle, kidney and ovary, but not in the liver, pancreas, lung or intestine. Therefore, no endogenous expression is expected to be observed and any ARK5 detected in the gastrointestinal organs (by Western blot) is from transfection of ARK5 plasmid.

In hypoxic conditions, AMP and Akt mediate tolerance. When deprived of glucose, for instance, the cell cycle G_1 phase is delayed and p53 phosphorylation increased by processes, which involve AMPK. Akt activates ARK5, which directly phosphorylates ATM, a member of the phosphoinositol-3 kinase (PI3K) family and activates the tumour suppressor p53 by phosphorylation at Ser[15] or through Chk2 at Ser[20] [during DNA damage]. This chain of events leads to cell cycle arrest or cell death. ARK5 and Akt co-immunoprecipitate, but separate just after Akt has been activated by either glucose starvation or insulin treatment. The dissociation enables ARK5-phosphorylation of ATM, as the ATM/p53 interaction is necessary to maintain survival during glucose starvation. Insulin activates Akt, which phosphorylates ARK5 and leads to activation of ATM and phosphorylates cell promoters, Bad

and caspase-9, thereby, inhibiting their biological function and inducing apoptosis via glucose starvation, TRAIL and TNF-α.

Wild type Akt and ARK5 have additive effects, suppressing cell death. Dominant negative Akt (DN-Akt) and/or ARK5 mutants cannot induce cell survival; therefore, ARK5 acts down-stream of Akt. ARK5 is the only AMPK member that responds to Akt, implicating it as the key mediator of tolerance to glucose starvation or insulin treatment.

2.8   Previous Studies

In an earlier Tannenbaum laboratory project, we evaluated the effects of glucosamine on macrophage activation functions using the murine macrophage cell line RAW 264.7. Macrophages are derived from bone marrow mononuclear phagocytic cells and the monocyte-macrophage system is actively involved in the elimination of various microorganisms, debris, dead cells and tissue during the cleaning of wounds (53). In addition to their phagocytic role, macrophages produce and secrete a number of enzymes that can act as cardinal cellular elements in inflammation and host resistance. Inclusion of the bacterial endotoxin (LPS) with macrophages, plus the cytokine, IFN-γ, up-regulates the expression of inflammatory molecules (such as TNF-α and iNOS) and, along with a boost in urea cycle enzymes, stimulates NO synthesis, leading to (8).

This project showed that the induction of TNF-α, NO, prostaglandin E2 (PGE2), COX2, and matrix metalloproteinase 9 (MMP9) by LPS and IFN-γ was reduced by the addition of glucosamine in a process that was modulated by ERK1/2 and JNK, but not by p38 MAPK or NFκB. It also identified ERK1/2 as being post-translationally modified by the addition of O-linked N-acetylglucosamine (O-GlcNAc). These findings suggest that glucosamine down-regulates macrophage activities through the use of signalling cascades, thus explaining its anti-inflammatory activity in OA. Moreover, glucosamine is implicated in the MAPK pathway, interacting with ERK1/2 and JNK, suggesting a role in apoptosis inhibition.

In a separate study, Kusakai, *et al*, (2004) introduced the ARK5 plasmid by transfection into the human hepatoma cell line, HepG2, and several colorectal cancer cell lines in efforts to protect cells against apoptosis (28).

Cells were exposed to the transfection reagent for four hours, yielding between 70% and 80% transfection, as measured by a green fluorescent protein (GFP) reporter. Transfection showed appreciable resistance to cell death, and the inclusion of the ARK5 plasmid into the cell's genome increased cell survival rate from 12.9% to 33.4% after 24 hours. This activity delayed the cell death, mediated by the mitochondrial death pathway.

3. RESEARCH DESIGN AND METHODOLOGY

The current study was designed to test the hypothesis: NO-protection from apoptosis is a universal mechanism, and to determine how to remove this NO-protection by manipulation of related pathways. The materials and procedures selected for this study are also justified. We identified appropriate cell types and treated them with a death-inducing agent, measuring apoptosis over a 24-hour time periods. We also inhibited independent variables that we presumed to have been embodied in the apoptotic pathway and observed changes in the cells' profiles.

3.1 Cell types

The use of cultured human tumour cells as model systems is an obvious first approach to experimental human research. The cell lines used in this study offer a preclinical opportunity to investigate the activity and properties of human cancer cells. We have selected systems that are fairly representative and approximate the physiological response of tumour cells *in vitro* and allow comparisons between cell types and between cancer types.

3.1-1 Prostate Cells: LNCaP

LNCaP cells express prostate-specific antigen (PSA) and prostatic acid phophatase (PAP) (58). Despite a low anchoring potential, the cells create monolayers in culture with a doubling time of 60-72 hours. They secrete and, thus, are response to polypeptide growth factors, especially EGF (54) and, with a high affinity androgen receptor, they are androgen-dependent. In contrast to this dependency, the addition of transforming growth factor beta (TGF-β) to the culture medium did not inhibit LNCaP proliferation. LNCaPs proved to be similarly resistant to the anitproliferative and antiviral effects of human interferon (HuIFNβ).

This finding is particularly important as a prospective therapeutic application in tumour treatment. The cells also have anchorage-independent proliferation in semisolid media and excellent cloning efficiency (18). Further, they produce poorly differentiated adenocarcinomas 14 to 56 days post-inoculation into nude mice, and form solid tumours in intact male hosts, but

21

not in their castrated male counterparts. The derivative sublines undergo phenotypic and genotypic changes irreversibly, and acquire androgen-independence and metastatic phenotypes when tested *in vivo* (26).

The androgen receptor has a mutation that allows oestradiol and progesterone to bind and stimulate LNCaP growth in the absence of oestrogen and progesterone receptors (55). The effects of the hormones show a biphasic dose-response relationship. Androgen sensitivity depends on culture conditions, as the cells adapt to the change in environment and often lose their biphasic dose-response.

3.1-2 Colon Cells: HT-29 and HCT-116

The first type of colon cancer cells used in our study was the colorectal adenocarcinoma, HT-29. This cell line retained its biological and physiological features of normal colorectal epithelium (38). As a malignant epithelial cell, it increased glucose consumption and lactate production with high levels of accumulated glycogen. HT-29 also expresses hormone and peptide receptors (notably, EGF-R), the receptors for insulin, vasoactive intestinal peptide (VIP) and prostaglandins. The study that produced these findings was conducted under culture conditions, where HT-29 cells are undifferentiated, while growing as a multilayer of unpolarised cells. They did not express cellular characteristics of any particular intestinal epithelial layer. However, under appropriate growth conditions, such as glucose and/or serum deprivation, HT-29 can be made to express differentiation characteristics.

One of the best indicators of a cell's tumourigenicity *in vitro* is its grouping into one of three classes (51), based on tumourigenicity, as seen by colony formation in soft agar. As a class I tumour-causing agent, the HT-29 cells produce palpable tumours ten days post-injection in 80% to 100% of injected mice. These tumours grow rapidly and at a uniform rate. The cells form multilayered colonies at plating efficiencies of between 25% and 30%. These cells arise from primary tumour site and grow to confluence in a monolayer pattern at a doubling time of 20 hours. However, the cell line is heterogeneous as it contains a small proportion (fewer than five per cent) of differentiated cells of either enterocytic or mucus-secreting type. They exhibited

weak expression of keratin, microvilli, tight junctions, zona adherens and desmosomes, which is indicative of their epithelial origin.

The HT-29 cells also secreted tumour-association markers, carcinoembryoinc antigen (CEA - 25 ng/10^6 cells), CA 19.9 (268 U/10^6 cells) and TGF-β binding protein (TGF-β-BP), the secretory product of IgA and mucin. CEA is considered to be a colon tumour-cell marker substance because high amounts of this antigen are found in colon carcinomas. For HT-29, CEA is found in the cell membrane and in the culture medium for even long-term cultures, and CEA is a principal member of a group soluble in percholic acid (57). These antigens do not show any effects of coordination.

Oncogene transcripts are detected in the growing medium of the cells. Specifically, c-myc, H-ras, K-ras, N-ras, Myb, fos, sis and p53 were found at the anticipated sizes. However, there is an additional sis-reactive band at 3.7 kilobase-pairs (kbp).

An additional colon cancer cell type, HCT-116, is derived from a primary human colon tumour and produces moderate mounts of CEA in tissue culture (1). The cells grow moderately well on soft agar. This colorectal carcinoma has a hMLH1 defective mismatch repair deficiency, which is relevant because most hereditary and sporadic colorectal cancers have deficiencies in MMR (27). The deficiency causes a higher spontaneous mutation rate, microsatellite instability, has more induced mutations in the hgpt locus, and increases the cells resistance to toxicity induced by 2-amino-1-methyl-6-phenylimidazo[4,5-b]pyridine (PhIP). This result suggests that PhIP-induced apoptosis is mediated through a MMR-dependent pathway. These cells have been associated with an increased resistance to chemotherapeutic agents, including cisplatin. However, MMR does not cause high-level resistance to cisplatin, doxorubicin or paclitaxel is not caused by MMR (31).

With respect to chemotherapeutic agents, the absence of hMLH1 curtailed arrest in the G2/M cell cycle phase and enhanced concomitant apoptosis with irinotecan (CPT-11), the standard treatment in colorectal cancer. Apoptosis induction happens independently of p53. There is a likelihood of an overlap between function of MMR and p53 in the activation of mutagenesis after an oxidative stress (29). Specifically, p53 and MMR cooperate to control

sensitivity to the cytotoxic effect and to limit its mutagenic potential in colon cancer cells. These cells are positive for keratin (by immunoperoxidase staining), transforming growth factor beta 1 and beta 2 (TGF-β1 and TGF-β2).

The cell viability of HCT-116 cells is relatively low. TRAIL triggers caspase-8 mediated truncation of BID and mitochondrial activation of caspase-9 in HCT-116, leading to apoptosis (22). Here, HCT-116 cells are Type II cells because their mitochondrial dependence and because TRAIL-induced apoptosis can be blocked by the caspase-9 inhibitor, Z-LEHD-FMK. Apoptotic signalling in HCT-116 depends on the doses and types of inducers, involving the bcl-2/bax family, death receptors, mitochondria and XIAP.

Even with variances across cell types, there is also heterogeneity in each cell population. These differences include morphology, state of differentiation, metastatic and invasive ability, karyotype, pharmacological response to drugs. Nevertheless, variant populations tend to retain their properties for extended periods of time (1). There are perceptible differences between *in vivo* and *in vitro* cultures with particularity towards the antigen secretion, generation time, morphology and tumourigenicity. With the exclusion of tumourigenicity, these properties are contingent upon the culture conditions, medium recipe, serum concentration and cell density. Tumourigenicity depends on, in addition to other factors, the inoculation route, cell dose and the presence of fibroblasts. Another important determinant is passage history. Prolonged cultivation *in vitro* can cause phenotypic drift, in which any potential offspring has properties distinct from the parent. Whereas these differences are apparent in CEA production, generation time, morphology and tumourigenicity, the HT-29 line has been synthesized for a number of years without losing its antigen secretion capacity (57).

3.2 Reagents and Protocols

We selected reagents and protocols because of their accuracy and ease of use. Often, the reagents and protocols were carried over from previous experiments, where they proved to be reliable.

3.2-1 Cell Growth Conditions

LNCaP cells were obtained from the Essigmann laboratory and maintained in RPMI 1640 medium with GlutaMAX acquired from GIBCO® (Grand Island, NY) and supplemented with 10% BioWhittaker™ heat inactivated foetal bovine serum, one per cent each of glucose, sodium pyruvate and HEPES from Sigma-Aldrich (Sheboygan Falls, WI).

HT-29 cells [from the Sorger laboratory] were similarly acquired and maintained in GIBCO® McCoy's 5A medium, supplemented with 10% heat inactivated foetal bovine serum from GIBCO® and one per cent each of BioWhittaker™ (Walkersville, MD) penicillin and streptomycin. HCT-116 cells were a generous donation from the Wogan laboratory, maintained in BioWhittaker™ McCoy's 5A medium and supplemented with Biosource (Camarillo, CA) 10% heat inactivated foetal bovine serum containing less than 0.06 EU/ml, by limulus amebocyte assay, and one per cent each of penicillin and streptomycin, also from BioWhittaker™. All cells were incubated at 37°C under five per cent CO_2.

Chemicals purchased from Sigma-Aldrich (St. Louis, MO) included: glucosamine, cycloheximide and N^G-monomethyl-L-arginine acetate salt (product number M7033). IFN-γ and the Cell Death Detection ELISA^{PLUS} assay were acquired from Roche (Indianapolis, IN). Recombinant human TNF-α was purchased from PeproTech (Rocky Hill, NJ). 1400W was purchased from Calbiochem (La Jolla, CA). Trypsin-EDTA (0.05% Trypsin with EDTA 4Na, 1X) and 1X phosphate-buffered saline (PBS) were also obtained from GIBCO®.

3.2-2 Cytokine Treatment of Cells

Cells were grown in appropriate media at 37°C, five per cent CO_2. At the time of the experiment, cells were trypsinised and plated at a density of $5*10^4$ cells/ml in 24-well, six-well or 10 cm dishes, with 0.5 ml, 1.5 ml or 10 ml cell suspension per well, respectively. After a 24-hour incubation period, the cells were incubated for 24 hours with 200 U/ml IFN-γ to stimulate iNOS induction, and subsequent to pre-treatment, we added other cytokines and glucosamine. (Previous experiments have shown that the most pronounced effects of glucosamine are observed when simultaneously added with cytokines and not hours before or after the cytokines.)

A dose response was done on all cells initially to determine the ideal concentration of death-inducing reagent that should be added to cause sufficient induction of apoptosis. Current literature prescribes that the typical concentrations used to induce apoptosis *in vitro* range between 25 ng/ml and 50 ng/ml and measured apoptosis after 24 hours. Thus, in administering our dose-response experimentation, we aimed toward observe the effects of TNF-α up to 100 ng/ml doses.

Preliminary data suggest that 50 ng/ml is the optimal level for testing. The cells were treated with TNF-α and/or glucosamine in final concentration of 2mM and, because we changed the medium at this stage, fresh IFN-γ is also added to the blend. In the NOS inhibitor experiments, 5 mM NMA or 20 μM 1400w was added at the induction of apoptosis. These concentrations were previously shown to sufficiently inhibit iNOS activity (23).

The cells were incubated for 24 hours with dose response or at the various times indicated in the graphs, and then trypsinised, rinsed with 1X PBS and collected at time of treatment or four, eight, 12, or 24 hours following treatment. The suspension is centrifuged at 6000 rpm for two minutes, after which the supernatant is removed and the cells frozen at –80°C overnight until the apoptosis assay was to be conducted.

3.2-3   Plasmid Preparation

ARK plasmids were obtained from the Esumi laboratory at the National Cancer Centre Research Institute, East. A common host strain, competent DH5α (*E. coli*) cells were used to propagate, express and isolate the plasmids prior to amplification. We thawed competent cells on ice and added 30 μl of the competent cells to each plasmid.

Tubes of the materials were gently tapped and incubated on ice for 30 minutes. Immediately following this step, we incubated the tubes at 42°C for 50 seconds as part of a heat shock to stimulate the cells to close their "pores", then snap-cooled them on ice for two minutes. To the plasmid DNA, we added 500 μl Luria Broth (LB – 10 g sodium chloride, 10 g tryptone, and 5 g yeast extract in one litre water). The tube was incubated at 37°C for one hour after which the mixture was spread on LB Agar Ampicillin plates, made with 12.5g

Agar in LB. After absorption of the mixture into the plate, it was incubated overnight (16 hours) at 37°C.

A single colony was then picked and inoculated with three millilitres of LB for eight hours. Five hundred microlitres of the mixture with a colony was mixed with 500 ml LB and grown to saturation at 37°C. The mixture was centrifuged at 6000 x g for 15 minutes at 4°C. The pellet was saved for the DNA maxiprep, administered according to manufacturer's protocol (Appendix B.1), with a QIAfilter Plasmid Maxi kit from QIAGEN (Valencia, CA). The plasmids were isolated and the cell lysates analysed in two per cent agarose gel with a one kbp ladder. In addition, the DNA concentration was measured and, to ensure purity of the samples, the optical density ratios were read on an Amersham Pharmacia Ultraspec 2100 pro UV/Visible spectrophotometer and corrected for scattered light at 320nm.

3.2-4   Transfection of ARK Plasmids into HT-29

ARK5 transfection into HT-29 cells was done with Invitrogen (Carlsbad, CA) Lipofectamine 2000 and Opti-MEM®I (GIBCO®) as per manufacturers' instructions (Appendix B.2). The procedure was optimised in 24-well plates with ratios of Lipofectamine™ 2000 (µl):DNA (µg) from a human recombinant green fluorescent protein expression plasmid from Stratagene (La Jolla, CA): of 1:1 to 4:1. Transfection efficiency was highest, as assessed by transfection with the GFP at a ratio of 1:2.5. Therefore, 0.8 µg DNA was used per 50 µl of Opti-MEM®I, giving a transfection efficiency of between 70% and 85%.

Transfection was done with GFP or one of three Ampicillin-resistant, G418-resistant plasmids: FLAG-ARK5 wildtype in pcDNA3.1(+) vector, ARK5 anti-sense (AS) in pcDNA3.1(-) and a dominant negative version of ARK5 (FLAG-DN-ARK5 S600A) in pcDNA3.1(+). After a four-hour exposure to the transfection mixtures, we replaced the growth medium on all cells with serum-containing McCoy's 5A. We allowed a one-day incubation at 37°C and five per cent CO_2, then pre-treated them for with IFN-γ for 24 hours and, thereafter added 200 nM insulin (Calbiochem) as a substrate for the Akt pathway. The cell death-induction [with TNF-α] and apoptosis detection were then carried out fully.

3.2-4 Detection of Apoptosis using an Immunocytochemical Assay

A key biochemical event during apoptosis is endonucleolysis -- cleavage of double stranded DNA at the most accessible internucleosomal linker region, generating mono- and oligonucleosomes. This endogenous reaction depends of calcium and magnesium concentrations. However, the DNA of the nucleosomes forms tight complexes with the core histones (H2A, H2B, H3 and H4), protecting it from cleavage by endonuclease. Therefore, the DNA fragments that form are discrete multiples of the 180 base-pair subunit, which can be detected as a "DNA-ladder" on agarose gels after extraction and separation of fragmented DNA. In the cytoplasm of the apoptotic cells, DNA degradation occurs several hours before the plasma membrane breaks down and there is a high concentration of the mono- and oligonucleosomes present.

The typical "DNA-ladder" on an agarose gel does not produce sufficient information about the histological localisation at the single cell level. An immunocytochemical assay and enzymatic labelling of apoptosis-induced DNA strand creaks (TUNEL) serve this purpose.

For this experiment, we chose to use the immunocytochemical assay with a mouse anti-DNA and anti-histone monoclonal antibodies, conjugated with peroxidase and biotin, respectively. The assay photometrically measured the relative quantities of histone and DNA that were present in the cytoplasm of cells after apoptosis was induced. The antibodies bound the histone component of the nucleosomes and simultaneously reacted with the immunocomplex to the streptavidin-coated multiplate through its biotinylation. The assay used quantitative determination of the amount of single- and double-stranded, low molecular weight DNA fragments retained in the immunocomplex by the POD, showing the internucleosomal degradation of genomic DNA during apoptosis. Meanwhile, the anti-histone-biotin antibody bound to the histones.

We opted for the modified ELISA was chosen because of its sensitivity and low background, and for its reliability in amplifying apoptosis. Also, it is a non-radioactive assay system, with easy handing and fast performance.

The cells were lysed with the lysis buffer included in the Cell Death Detection ELISA^{PLUS} kit. After a one-half hour of incubation at room

temperature and centrifugation at 200 x *g* for 10 minutes, the protein concentration of the supernatant was measured with the BCA protein assay kit (Pierce, Rockford, IL), as per manufactures' instructions. From this value were determined the relative amount of apoptosis per mg of protein used to normalise the data to the total protein concentrations of each sample. This measurement/calculation allowed for observation of the effects of cytokine treatment on both the relative apoptosis levels and cell division.

The Roche assay was continued by carefully transferring 20 µl of the supernatant into the streptavidin-coated multiplate and adding 80 µl of the Immunoreagent to each well. The remaining elements of the procedure were consistent with those suggested by the manufacturer (Appendix B.3). After the absorbances were taken, the values were averaged and the background value is subtracted from this average. Then, the specific enrichment of mono- and oligonucleosomes released into the cytoplasm was calculated using the equation below:

$$\text{Fold Apoptosis} = \frac{\text{Absorption of sample (dying/dead cells)}}{\text{Absorption of corresponding negative control}} \qquad \textbf{(Equation 5)}$$

Exponentially growing permanent cell cultures contain a certain amount of dead cells, usually approximately 3-8%. In this immunoassay, the inherent dead cells in the untreated sample (without TNF-α inducing cell death) result in a certain absorbance value, which, depending on the amount of dead cells, may even exceed the absorption value of the immunoassay background.

29

4. EVALUATION

The study results provide an objective basis for testing our hypothesis, given the incidence of cancer death, our work was exploratory as we sought to learn more about the effects of nitric oxide and it inhibits distinct from the results of the transfection and glucosamine experiments.

4.1 Nitric Oxide Protects all Cancer Cells against Apoptosis

We explored the mechanism of apoptosis in colorectal and prostate cancer cells to validate our belief that (a) cancer cells and protected from apoptosis by S-nitrosation, and (b) this mechanism is not unique to the colorectal cells, HT-29. Our goals were to enhance understanding of NO protection from apoptosis.

Data obtained from duplicate trials [during our study] help to propose a means of circumventing the mechanism and, correspondingly, offers opportunities for additional investigation.

4.1-1 Apoptosis Induction in Cells

The action of controlling apoptosis in cancer cells was challenging and warranted a four-prong approach. First, we determined the appropriate dose of death-inducing agent to elicit a sufficiently distinct response that is characteristic of apoptosis with the ultimate goal of establishing the dose at which half the cells undergo apoptosis (LD_{50}). Next, we fitted the data to sigmoid equations, as with the typical dose response, as follows:

$$y = \frac{a}{1 + e^{-bx}} \qquad \textbf{(Equation 6)}$$

Where, $a_1 = 2.62$ and $b_1 = 0.28$ for LNCaPs, and $a_2 = 4.99$ and $b_2 = 0.86$ for the HCT-116 with TNF-α and IFN-γ.

As illustrated by the steep slopes in Figure 6, TNF-α is very toxic in low doses to the LNCaP and HCT-116 cancer cells. The dose response curves, surprisingly, showed dramatic effects at and above 1ng/ml of TNF-α. Consequently, the LD_{50} values for both cell types hovered below 1 ng/ml and,

from the best-fit graphs, are in the "pico-" range. TNF-α concentrations above the 5 ng/ml and 10 ng/ml in HCT-116 and LNCaP cells, respectively, have little variance (including standard error) in response to the cells. By implication, the number of cells observed under apoptosis above these concentrations does not vary in any significant way. The literature indicates that apoptosis is typically induced in cancer cells with 25-50 ng/ml of TNF-α. To confirm such and outcome, we bombarded the cells with the death-inducing agent and decided that, given the results from Kim, *et al*, the ideal concentration to induce apoptosis in the cell lines approached the literature-prescribed concentration. Therefore, the cells were treated with 50 ng/ml.

Literature on apoptosis in HCT-116 cells explains the synergistic cytotoxic effects of 10 ng/ml of TNF-α and 10 ng/ml of IFN-γ, reducing the number of cell colonies by 89% (43). Park, *et al*, (41) also demonstrated that priming LNCaP cells with 200 U/ml IFN-γ enhances the effectiveness of TNF-α in inducing apoptosis. We confirmed these observations with 24-hour pre-treatment of IFN-γ. Our results indicated that TNF-α alone produced moderate levels of apoptosis and that fold apoptosis is three times higher when TNF-α is used in conjunction with IFN-γ. For this reason, both cytokines are added to the medium to stimulate apoptosis in subsequent experiments with HCT-116 and LNCaP cells.

Our second objective was to induce death with a cytokine mixture of TNF-α and IFN-γ and observe the cellular response over a 24-hour period. The response in HT-29 cells (Figure 7) comported with those of the other cells, indicating that TNF-α and IFN-γ alone induce little apoptosis; their co-stimulatory effects are more pronounced with 18-fold apoptosis at 24 hours. This procedure induced apoptosis indeed earlier for the colon cancer cells than for the prostate cancer cells. HCT-116 cells show a rapid increase in apoptosis within four hours (Figure 7b) while the HT-29 cells have a maximal response after eight hours. For both these cell types, the initial spike is followed by a small decrease of 6% for HCT-116 and 18% for HT-29. The change probably reflected one successful cell division (over the course of incubation) and an increase in cell number thus, decreasing the relative fold apoptosis in a background of newly formed cells. In LNCaP cells, the response is gradual up to 24 hours, at which point, the fold apoptosis in the cells is much higher.

31

Hence, the effects of the NOS inhibitors and glucosamine in LNCaP cells, if any, will probably be evident closer to 24 hours of incubation.

4.1-2   Effect of NOS Inhibitors

The NOS inhibitors were added to the cytoplasm at the time of apoptosis induction as the effects were expected to occur over a similar timeline as TNF-α. Their anticipated action was to remove the nitric oxide protection of cells from apoptosis. In part three of our study, NMA accomplished the expected results. It increased apoptosis in LNCaP cells over the course of 24 hours and, at which point, there was 40% more apoptosis in NMA-treated, death-induced cells (Figure 8). Similarly, in HCT-116 cells, NMA caused, on the average, 30% more apoptosis in death-induced cells. These results confirmed the findings by Kim, et al, in which NMA increased apoptosis. The Kim study also determined that the mechanism of action involved enhanced caspase-9, caspase-3 and PARP cleavage and activity. We concluded that these pathways were not cell-specific and that the reaction seen in the present experiments occurred via a similar mechanism in the HCT-116 and LNCaP cells.

Another inhibitor, 1400W, was used to corroborate the results and further explicate the role of NOS in the process. Unlike NMA, 1400W is believed to selectively inhibit iNOS activity; thus, changes due to NO synthesis should, in the presence of 1400W, reflect constitutive expression. In Figure 9, 1400W appeared to cause a slight increase in the amount of apoptosis in HCT-116 cells but the change is only 10% and is considered negligible. In LNCaP cells, a reverse is trend observed. That is, 1400W seemingly reduces apoptosis, but, again, only insignificantly. We believe that this NOS inhibitor had practically no effect on apoptosis in the cell types; therefore, we cannot conclude that the changes seen with NOS inhibitors are iNOS-specific. These results contradict Kim, et al, who had stated a notable increase in apoptosis in HT-29 cells.

The results of NMA-inhibition of NOS and subsequent reduction in apoptosis support our hypothesis, NO protects cells from apoptosis via S-nitrosation and that inhibiting NO would remove this protection and increase apoptosis. However, the results with 1400W are unconvincing with conflicting outcomes in the different cell lines. As an iNOS-specific inhibitor, 1400w was

expected to increase apoptosis, indicating that the source of NOS is inducible or have no material effect on constitutive NOS production. Regardless, we successfully reduced apoptosis by inhibiting NO synthesis with NMA, and these results are potentially useful in the effort to regulate apoptosis in cancer cells.

4.1-3   Transfection and TNF-a induced Apoptosis

A relatively small fraction of the underlying cells incorporate the DNA and, of those, fewer have insertions that do not disrupt essential genes. To ensure a successful incorporation of the plasmids into the cells' genome, we optimised the experimentation with GFP. At a Lipofectamine™ 2000 (µl):DNA (µg) ratio of 2:1, the GFP was appropriately transfected into the HT-29 cells at a frequency of 75%. Higher ratios showed no marked increase in the transfection efficiency, so the concentration used in the remaining the experiment was 0.8 µg of GFP. In the plasmid transformation, the non-transformed, control culture produced no colonies, and this indicated that Ampicillin inhibited growth of *E. coli* without the plasmid. Gel electrophoresis indicated that the inserts were of the correct and expected size at 6.8 kbp. The transformation and amplification were successful, and optical density measurements are reported in Table 2.

Esumi, *et al*, had shown that ARK5 plasmid transfection into colorectal cancer cells inhibited TNF-α induced apoptosis. Fold apoptosis was determined, as mentioned above, from the ELISA assay and Equation 5. Figure 10 reveals no trend in ARK5 protection against cell death. In fact, insertion of ARK5 plasmids and GFP into HT-29 colon cancer cells yields similar effects on the relative cell death, increasing apoptosis upwards of four-fold. Control cells further reveal three important points: treatment with the cytokines induced apoptosis, cytokine synergism is maintained in this background, and the addition of insulin had no effect on degree of cell death.

We expected ARK5 transfection to protect the cells from apoptosis. The dominant negative and anti-sense forms should cause more apoptosis because the DN would knock down ARK5 activity, while the AS produces complimentary strands that inhibit active ARK5. The ARK5 plasmid could have inserted downstream of inactive promoter, but this is unlikely to have happened for all successful insertions (that is, not inserting in essential genes). Alternatively,

and more likely, the transfection process probably caused some apoptosis and, above this "baseline" apoptotic level, ARK5 shows no protective effect. Moreover, one cannot distinguish between an ARK5-induced decrease in apoptosis and a disruption of delicate balance of cellular activity by transfection procedure, resulting in [TNF-α-independent] cell death. In Esumi, *et al*, several colorectal cells with similar characteristics to those as HT-29 cells are investigated. Theoretically, the HT-29 cells should produce similar results and, based on the results, one cannot conclude that the ARK5 plasmid protects these cells from apoptosis.

4.2   Glucosamine Reduces Cytokine-induced Apoptosis

We investigated the effect of a proven MAPK inhibitor on apoptosis and present the results in Figure 11. Treatment comprised of 50 ng/ml TNF-α induced apoptosis in HCT-116 cells, beginning four hours and up to a maximum of eight-fold after 24 hours. The addition of 2mM glucosamine to the cells reduced by an average of 30% the maximum level of apoptosis that is observed in these cells over the time course. The effects are noted early. However, the control cells showed a change of three-fold over time, compromising the credibility of the results. Glucosamine has a less marked effect on LNCaP cells, since it reduces apoptosis by 15% after 24 hours of incubation. The trend begins to develop around eight hours and indicates a slowdown in the rate at which apoptosis begins and occurs in the prostate cancer cells treated with glucosamine. These values are not significant to consider glucosamine as having an effect on the LNCaP cells. The control and glucosamine-treated cells show no appreciate change in the fold apoptosis over the 24-hour time period.

The response by HT-29 is equally puzzling. Glucosamine seemingly increases apoptosis in the short term (up to the 12-hour time point), where cells treated with glucosamine show more 20% apoptosis. After 12 hours, the amount of apoptosis in glucosamine-treated cells plunges, but the final 24-hour fold apoptosis lies inconsequentially lower than that for the control cells.

Our team has shown that glucosamine is an ERK1/2 inhibitor; it should decrease the amount of apoptosis because MAP kinases are involved in

34

apoptosis, preventing AP-1 and NFκB activation. The response in HCT-116 cells positively confirms these expectations, but the other cell types show conflicting effects. These results are inconclusive in that the effects of glucosamine in colon and prostate cancer cells are uncertain. Further investigation would help to determine whether the reduction in apoptosis, observed in HCT-cells is an artefact. One possible explanation for these results hinges on the use of a high concentration of glucosamine in these experimentations, though the typical concentration range of glucosamine is between 10 μM and 3 mM.

Previously, experiments done were with RAW 264.7 macrophages in which the cells were treated for eight hours with 100 ng/ml LPS, 50 U/ml IFN-γ and, simultaneously, varying concentrations of glucosamine. Changes in the nitric oxide concentration were monitored by the analysis of media samples for the stable degradation product, nitrite, with use of the standard colorimetric Griess reaction (60). This study proved that 2 mM glucosamine neither depletes ATP nor alters physiology of relevant pathways that define the cells' response to the death-inducing agent (data not shown). In addition, this concentration elicited a drastic reduction of 94% in nitrite production as a result of NOS activity (Figure 12). This trend was readily discernible and, for the purposes of the underlying experimentations, we deemed it suitable. Despite the suitability of a high concentration, the results from the glucosamine studies are in dissent.

5. CONCLUSIONS AND RECOMMENDATIONS

Cancer incidence rates have stabilised over the past five years, due in part to the Centres for Disease Control's public awareness initiative. Cancer mortality for women has declined by 1.5% per year since 1993, and for men it fell by 0.8% per year since 1992 (20). For those who already suffer from cancer, chemotherapy is their primary form of treatment. This therapy indiscriminately kills cells, so the current drive is for to identify alternative therapies that target cancer cells.

Our study sought to determine whether findings [of S-nitrosation in colorectal cells] by Kim, *et al*, (2004) are applicable to other cell types. Our approach was to investigate, synthesise conclusions and exploit the mechanisms that cancer cells use to avoid normal signals for cell death, specifically apoptosis. Kim and her team proved that NO protects the colorectal cancer cell line, HT-29, from apoptosis in a process called S-nitrosation. Our own investigation supports the hypothesis: HT-29 cells are not unique in their response to nitric oxide inhibitors, and NO-protection from apoptosis is not specific to this cell line. They showed that NO actually protects many types of cancer cells from apoptosis and that inhibition of NO leads to increased cell death.   Further, the mechanism by which NO inhibits apoptosis may be universal, meaning that it operates in other colorectal cells and in prostate cancer cells, too. An important inference is that treatments for cancer patients can be constructed to target NO inhibition to the tumour. Our laboratory experience with the iNOS inhibitor, 1400W, suggests that these cancer cell-specific treatments would not involve the inhibition of inducible NOS.

Glucosamine did not support the notion that apoptosis can be reduced via MAPK inhibition. Hence, we can postulate that the mechanism of TNF-α-induced apoptosis proceeds independently of the MAPK pathways that involve ERK1/2. We could not ascertain whether the ARK5 plasmid currently is a feasible source of treatment because the effects of ARK5 do not facilitate observation in a background of transfection-induced apoptosis. The problem be appropriately linked to the time lab between the plasmid input and cytokine treatment. The plasmid is not transferable to offspring, so mitotic division produces cells that do not have the plasmid in their genome. If indeed the

ARK5 response is characteristic of HT-29 cells, this method currently offers no protection for these cells from TNF-α-induced apoptosis.

Given the evidence and evaluation presented in this paper as part of our efforts, we hope that there will be additional work, using mice for in vivo studies with the infusion of NMA into tumours and observing subsequent changes to the size or characteristics of the tumours. Other potential techniques for consideration include proteomic investigation into the effects of NOS inhibitors and glucosamine. In our introduction, we cited the challenges associated with controlling disease. We hope that the research discussed in this paper represents a useful step in the path toward developing drugs to control, if not cure cancer.

6. REFERENCES

1. Brattain, M. G., D. E. Brattain, A. M. Sarrif, L. J. McRae, W. D. Fine, and J. G. Hawkins. 1982. Enhancement of growth of human colon tumor cell lines by feeder layers of murine fibroblasts. J Natl Cancer Inst 69:767-771.

2. Brown, G. C. 1999. Nitric oxide and mitochondrial respiration. Biochim Biophys Acta 1411:351-369.

3. Chan, E. D., B. W. Winston, S. T. Uh, L. K. Remigio, and D. W. Riches. 1999. Systematic evaluation of the mitogen-activated protein kinases in the induction of iNOS by tumor necrosis factor-alpha and interferon-gamma. Chest 116:91S-92S.

4. Cohen, G. M. 1997. Caspases: the executioners of apoptosis. Biochem J 326 (Pt 1):1-16.

5. Cuzzocrea, S., B. Zingarelli, P. Hake, A. L. Salzman, and C. Szabo. 1998. Antiinflammatory effects of mercaptoethylguanidine, a combined inhibitor of nitric oxide synthase and peroxynitrite scavenger, in carrageenan-induced models of inflammation. Free Radic.Biol.Med. 24:450-459.

6. Denicola, A. and R. Radi. 2005. Peroxynitrite and drug-dependent toxicity. Toxicology 208:273-288.

7. Du, C., M. Fang, Y. Li, L. Li, and X. Wang. 2000. Smac, a mitochondrial protein that promotes cytochrome c-dependent caspase activation by eliminating IAP inhibition. Cell 102:33-42.

8. Ehrt, S., D. Schnappinger, S. Bekiranov, J. Drenkow, S. Shi, T. R. Gingeras, T. Gaasterland, G. Schoolnik, and C. Nathan. 2001. Reprogramming of the macrophage transcriptome in response to interferon-gamma and Mycobacterium tuberculosis: signaling roles of nitric oxide synthase-2 and phagocyte oxidase. J Exp.Med. 194:1123-1140.

9. Feelisch, M., T. Rassaf, S. Mnaimneh, N. Singh, N. S. Bryan, D. Jourd'Heuil, and M. Kelm. 2002. Concomitant S-, N-, and heme-nitros(yl)ation in biological tissues and fluids: implications for the fate of NO in vivo. FASEB J 16:1775-1785.

10. Felson, D. T. and T. E. McAlindon. 2000. Glucosamine and chondroitin for osteoarthritis: to recommend or not to recommend? Arthritis Care Res 13:179-182.

11. Garvey, E. P., J. A. Oplinger, E. S. Furfine, R. J. Kiff, F. Laszlo, B. J. Whittle, and R. G. Knowles. 1997. 1400W is a slow, tight binding, and highly selective inhibitor of inducible nitric-oxide synthase in vitro and in vivo. J Biol.Chem 272:4959-4963.

12. Garvey, E. P., J. A. Oplinger, G. J. Tanoury, P. A. Sherman, M. Fowler, S. Marshall, M. F. Harmon, J. E. Paith, and E. S. Furfine. 1994. Potent and selective inhibition of human nitric oxide synthases. Inhibition by non-amino acid isothioureas. J Biol.Chem 269:26669-26676.

13. Gaston, B. 1999. Nitric oxide and thiol groups. Biochim Biophys Acta 1411:323-333.

14. Gaston, B. M., J. Carver, A. Doctor, and L. A. Palmer. 2003. S-nitrosylation signaling in cell biology. Mol.Interv. 3:253-263.

15. Gouze, J. N., A. Bianchi, P. Becuwe, M. Dauca, P. Netter, J. Magdalou, B. Terlain, and K. Bordji. 2002. Glucosamine modulates IL-1-induced activation of rat chondrocytes at a receptor level, and by inhibiting the NF-kappa B pathway. FEBS Lett. 510:166-170.

16. Hengartner, M. O. 2000. The biochemistry of apoptosis. Nature 407:770-776.

17. Hess, D. T., A. Matsumoto, S. O. Kim, H. E. Marshall, and J. S. Stamler. 2005. Protein S-nitrosylation: purview and parameters. Nat.Rev.Mol.Cell Biol. 6:150-166.

18. Horoszewicz, J. S., S. S. Leong, E. Kawinski, J. P. Karr, H. Rosenthal, T. M. Chu, E. A. Mirand, and G. P. Murphy. 1983. LNCaP model of human prostatic carcinoma. CANCER RES 43:1809-1818.

19. Inerot, S., D. Heinegard, L. Audell, and S. E. Olsson. 1978. Articular-cartilage proteoglycans in aging and osteoarthritis. Biochem J 169:143-156.

20. Jemal, A., T. Murray, E. Ward, A. Samuels, R. C. Tiwari, A. Ghafoor, E. J. Feuer, and M. J. Thun. 2005. Cancer statistics, 2005. CA Cancer J Clin. 55:10-30.

21. Jun, C. D., H. O. Pae, H. J. Kwak, J. C. Yoo, B. M. Choi, C. D. Oh, J. S. Chun, S. G. Paik, Y. H. Park, and H. T. Chung. 1999. Modulation of nitric oxide-induced apoptotic death of HL-60 cells by protein kinase C and protein kinase A through mitogen-activated protein kinases and CPP32-like protease pathways. Cell Immunol. 194:36-46.

22. Kim, D. M., S. Y. Koo, K. Jeon, M. H. Kim, J. Lee, C. Y. Hong, and S. Jeong. 2003. Rapid induction of apoptosis by combination of flavopiridol and tumor necrosis factor (TNF)-alpha or TNF-related apoptosis-inducing ligand in human cancer cell lines. CANCER RES 63:621-626.

23. Kim, J. E. and S. R. Tannenbaum. 2004. S-Nitrosation regulates the activation of endogenous procaspase-9 in HT-29 human colon carcinoma cells. J Biol.Chem 279:9758-9764.

24. Kim, P. K., Y. G. Kwon, H. T. Chung, and Y. M. Kim. 2002. Regulation of caspases by nitric oxide. Ann.N.Y.Acad Sci 962:42-52.

25. Kim, P. K., R. Zamora, P. Petrosko, and T. R. Billiar. 2001. The regulatory role of nitric oxide in apoptosis. Int.Immunopharmacol. 1:1421-1441.

26. Koeneman, K. S., F. Yeung, and L. W. Chung. 1999. Osteomimetic properties of prostate cancer cells: a hypothesis supporting the predilection of prostate cancer metastasis and growth in the bone environment. Prostate 39:246-261.

27. Koi, M., A. Umar, D. P. Chauhan, S. P. Cherian, J. M. Carethers, T. A. Kunkel, and C. R. Boland. 1994. Human chromosome 3 corrects mismatch repair deficiency and microsatellite instability and reduces N-methyl-N'-nitro-N-nitrosoguanidine tolerance in colon tumor cells with homozygous hMLH1 mutation. CANCER RES 54:4308-4312.

28. Kusakai, G., a. Suzuki, T. Ogura, S. Miyamoto, A. Ochiai, M. Kaminishi, and H. Esumi. 2004. ARK5 expression in colorectal cancer and its implications for tumor progression. Am.J Pathol. 164:987-995.

29. Lin, X., K. Ramamurthi, M. Mishima, A. Kondo, and S. B. Howell. 2000. p53 interacts with the DNA mismatch repair system to modulate the cytotoxicity and mutagenicity of hydrogen peroxide. Mol.Pharmacol. 58:1222-1229.

30. Lipton, S. A., Y.-B. Choi, Z.-H. Pan, S. Z. Lei, H.-S. Vincent Chen, N. J. Sucher, J. Loscalzo, D. J. Singel, and J. S. Stamler. 1993. A redox-based mechanism for the neuroprotective and neurodestructive effects of nitric oxide and related nitroso-compounds. Nature 364:626-632.

31. Liu, L., P. Taverna, C. M. Whitacre, S. Chatterjee, and S. L. Gerson. 1999. Pharmacologic disruption of base excision repair sensitizes mismatch repair-deficient and -proficient colon cancer cells to methylating agents. Clin.Cancer Res 5:2908-2917.

32. Lockshin, R. A. and Z. Zakeri. 2004. Apoptosis, autophagy, and more. Int.J Biochem Cell Biol. 36:2405-2419.

33. Marletta, M. A., P. S. Yoon, R. Iyengar, C. D. Leaf, and J. S. Wishnok. 1988. Macrophage oxidation of L-arginine to nitrite and nitrate: nitric oxide is an intermediate. Biochemistry 27:8706-8711.

34. Marshall, H. E., K. Merchant, and J. S. Stamler. 2000. Nitrosation and oxidation in the regulation of gene expression. FASEB J 14:1889-1900.

35. Meininger, C. J., K. A. Kelly, H. Li, T. E. Haynes, and G. Wu. 2000. Glucosamine inhibits inducible nitric oxide synthesis. Biochem Biophys.Res Commun. 279:234-239.

36. Miranda, K. M., R. W. Nims, D. D. Thomas, M. G. Espey, D. Citrin, M. D. Bartberger, N. Paolocci, J. M. Fukuto, M. Feelisch, and D. A. Wink. 2003. Comparison of the reactivity of nitric oxide and nitroxyl with heme proteins. A chemical discussion of the differential biological effects of these redox related products of NOS. J Inorg.Biochem 93:52-60.

37. Moon, S. K., B. Y. Cha, and C. H. Kim. 2004. ERK1/2 mediates TNF-alpha-induced matrix metalloproteinase-9 expression in human vascular smooth muscle cells via the regulation of NF-kappaB and AP-1: Involvement of the ras dependent pathway. J Cell Physiol 198:417-427.

38. Morin, P. J., B. Vogelstein, and K. W. Kinzler. 1996. Apoptosis and APC in colorectal tumorigenesis. Proc Natl Acad Sci U S A 93:7950-7954.

39. Morris, K. R., R. D. Lutz, H. S. Choi, T. Kamitani, K. Chmura, and E. D. Chan. 2003. Role of the NF-kappaB signaling pathway and kappaB cis-regulatory elements on the IRF-1 and iNOS promoter regions in

mycobacterial lipoarabinomannan induction of nitric oxide. Infect.Immun. 71:1442-1452.

40. Padgett, C. M. and A. R. Whorton. 1998. Cellular responses to nitric oxide: role of protein S-thiolation/dethiolation. Arch.Biochem Biophys. 358:232-242.

41. Park, S. Y., J. W. Seol, Y. J. Lee, J. H. Cho, H. S. Kang, I. S. Kim, S. H. Park, T. H. Kim, J. H. Yim, M. Kim, T. R. Billiar, and D. W. Seol. 2004. IFN-gamma enhances TRAIL-induced apoptosis through IRF-1. Eur.J Biochem 271:4222-4228.

42. Rao, C. V. 2004. Nitric oxide signaling in colon cancer chemoprevention. MUTAT RES 555:107-119.

43. Schiller, J. H., G. Bittner, B. Storer, and J. K. Willson. 1987. Synergistic antitumor effects of tumor necrosis factor and gamma-interferon on human colon carcinoma cell lines. CANCER RES 47:2809-2813.

44. Singh, R. J., N. Hogg, J. Joseph, and B. Kalyanaraman. 1996. Mechanism of nitric oxide release from S-nitrosothiols. J Biol.Chem 271:18596-18603.

45. Southan, G. J., C. Szabo, and C. Thiemermann. 1995. Isothioureas: potent inhibitors of nitric oxide synthases with variable isoform selectivity. Br.J Pharmacol. 114:510-516.

46. Southan, G. J., B. Zingarelli, M. O'Connor, A. L. Salzman, and C. Szabo. 1996. Spontaneous rearrangement of aminoalkylisothioureas into mercaptoalkylguanidines, a novel class of nitric oxide synthase inhibitors with selectivity towards the inducible isoform. Br.J Pharmacol. 117:619-632.

47. Studer, R. K., H. I. Georgescu, L. A. Miller, and C. H. Evans. 1999. Inhibition of transforming growth factor beta production by nitric oxide-treated chondrocytes: implications for matrix synthesis. Arthritis Rheum. 42:248-257.

48. Suzuki, a., G. Kusakai, A. Kishimoto, J. Lu, T. Ogura, and H. Esumi. 2003. ARK5 suppresses the cell death induced by nutrient starvation and death receptors via inhibition of caspase 8 activation, but not by chemotherapeutic agents or UV irradiation. Oncogene 22:6177-6182.

49. Suzuki, a., G. Kusakai, A. Kishimoto, J. Lu, T. Ogura, M. F. Lavin, and H. Esumi. 2003. Identification of a novel protein kinase mediating Akt survival signaling to the ATM protein. J Biol.Chem 278:48-53.

50. Towheed, T. E. 2003. Current status of glucosamine therapy in osteoarthritis. Arthritis Rheum. 49:601-604.

51. Trainer, D. L., T. Kline, F. L. McCabe, L. F. Faucette, J. Feild, M. Chaikin, M. Anzano, D. Rieman, S. Hoffstein, D. J. Li, and . 1988. Biological characterization and oncogene expression in human colorectal carcinoma cell lines. Int.J Cancer 41:287-296.

52. Tufan, A. C., K. M. Daumer, A. M. DeLise, and R. S. Tuan. 2002. AP-1 transcription factor complex is a target of signals from both WnT-7a and N-cadherin-dependent cell-cell adhesion complex during the regulation of limb mesenchymal chondrogenesis. Exp.Cell Res 273:197-203.

53. Unanue, E. R., D. I. Beller, J. Calderon, J. M. Kiely, and M. J. Stadecker. 1976. Regulation of immunity and inflammation by mediators from macrophages. Am.J Pathol. 85:465-478.

54. van Steenbrugge, G. J., C. J. van Uffelen, J. Bolt, and F. H. Schroder. 1991. The human prostatic cancer cell line LNCaP and its derived sublines: an in vitro model for the study of androgen sensitivity. J Steroid Biochem Mol.Biol. 40:207-214.

55. Veldscholte, J., C. A. Berrevoets, and E. Mulder. 1994. Studies on the human prostatic cancer cell line LNCaP. J Steroid Biochem Mol.Biol. 49:341-346.

56. Verhagen, A. M., P. G. Ekert, M. Pakusch, J. Silke, L. M. Connolly, G. E. Reid, R. L. Moritz, R. J. Simpson, and D. L. Vaux. 2000. Identification of DIABLO, a mammalian protein that promotes apoptosis by binding to and antagonizing IAP proteins. Cell 102:43-53.

57. von Kleist, S., E. Chany, P. Burtin, M. King, and J. Fogh. 1975. Immunohistology of the antigenic pattern of a continuous cell line from a human colon tumor. J Natl Cancer Inst 55:555-560.

58. Webber, M. M., D. Bello, and S. Quader. 1997. Immortalized and tumorigenic adult human prostatic epithelial cell lines: characteristics and applications Part 2. Tumorigenic cell lines. Prostate 30:58-64.
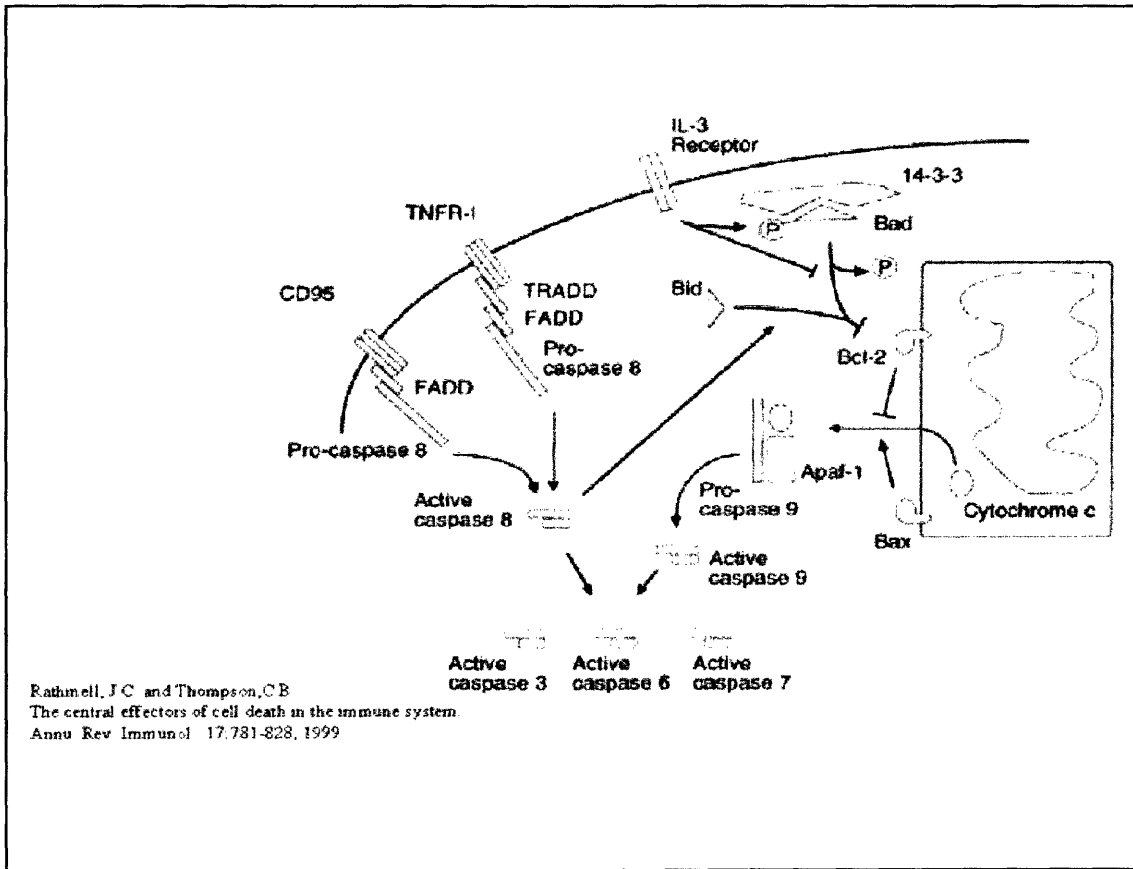
43

59. Wesemann, D. R. and E. N. Benveniste. 2003. STAT-1 alpha and IFN-gamma as modulators of TNF-alpha signaling in macrophages: regulation and functional implications of the TNF receptor 1:STAT-1 alpha complex. J Immunol. 171:5313-5319.

60. Wishnok, J. S., J. A. Glogowski, and S. R. Tannenbaum. 1996. Quantitation of nitrate, nitrite, and nitrosating agents. Methods Enzymol. 268:130-141.

61. Wu, G., T. E. Haynes, H. Li, W. Yan, and C. J. Meininger. 2001. Glutamine metabolism to glucosamine is necessary for glutamine inhibition of endothelial nitric oxide synthesis. Biochem J 353:245-252.

62. Zhang, G. and S. Ghosh. 2002. Negative regulation of toll-like receptor-mediated signaling by Tollip. J Biol.Chem 277:7059-7065.

APPENDIX A. FIGURES

The symbols used through Appendix A are consistent and adhere to the following legend:

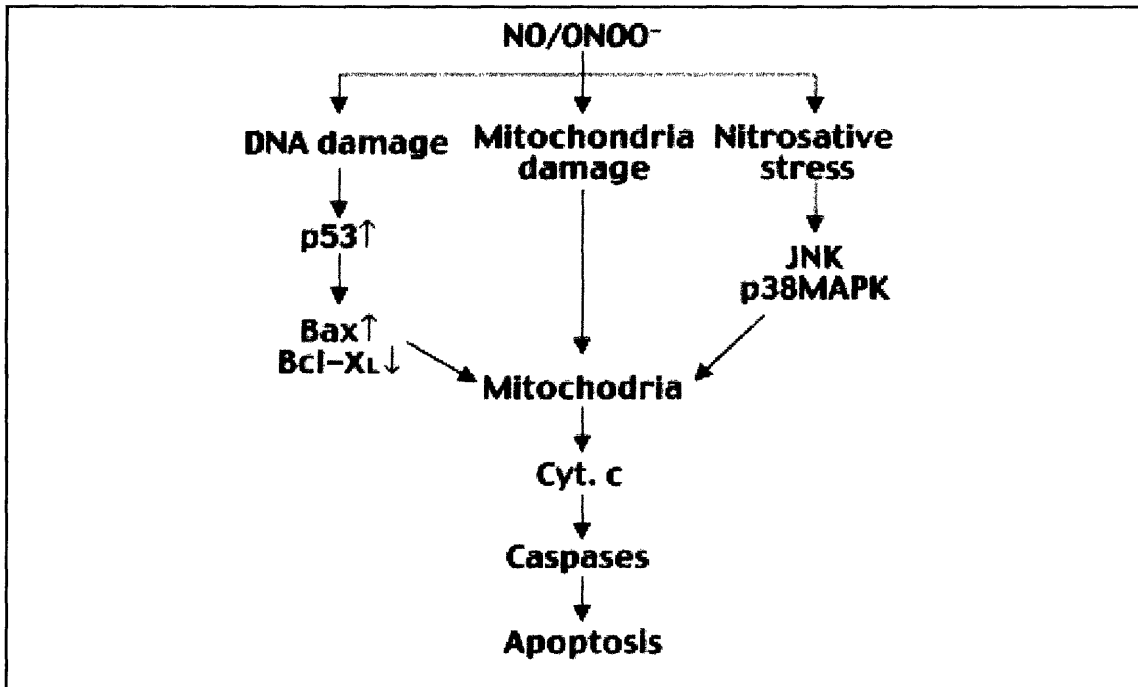**Table 1. Legend of Symbols Used in the Figures**

Symbol	Condition
●	Control
☐	200 U/ml IFN-γ
✕	50 ng/ml TNF-α
■	200 U/ml IFN-γ + 50 ng/ml TNF-α
◇	5 mM NMA
◆	5 mM NMA + 200 U/ml IFN-γ + 50 ng/ml TNF-α
△	20 µM 1400W
▲	20 µM 1400W + 200 U/ml IFN-γ + 50 ng/ml TNF-α
○	2 mM GlcN
●	2 mM GlcN + 200 U/ml IFN-γ + 50 ng/ml TNF-α

IL-3
Receptor

14-3-3

TNFR-1

Bad

(P)

(P)

CD95

TRADD
FADD

Bid

Pro-
caspase 8

Bcl-2

FADD

Pro-caspase 8

Apaf-1

Pro-
caspase 9

Cytochrome c

Active
caspase 8

Bax

Active
caspase 9

Active
caspase 3

Active
caspase 6

Active
caspase 7

Figure 1. Caspase Activation by Surface Receptors
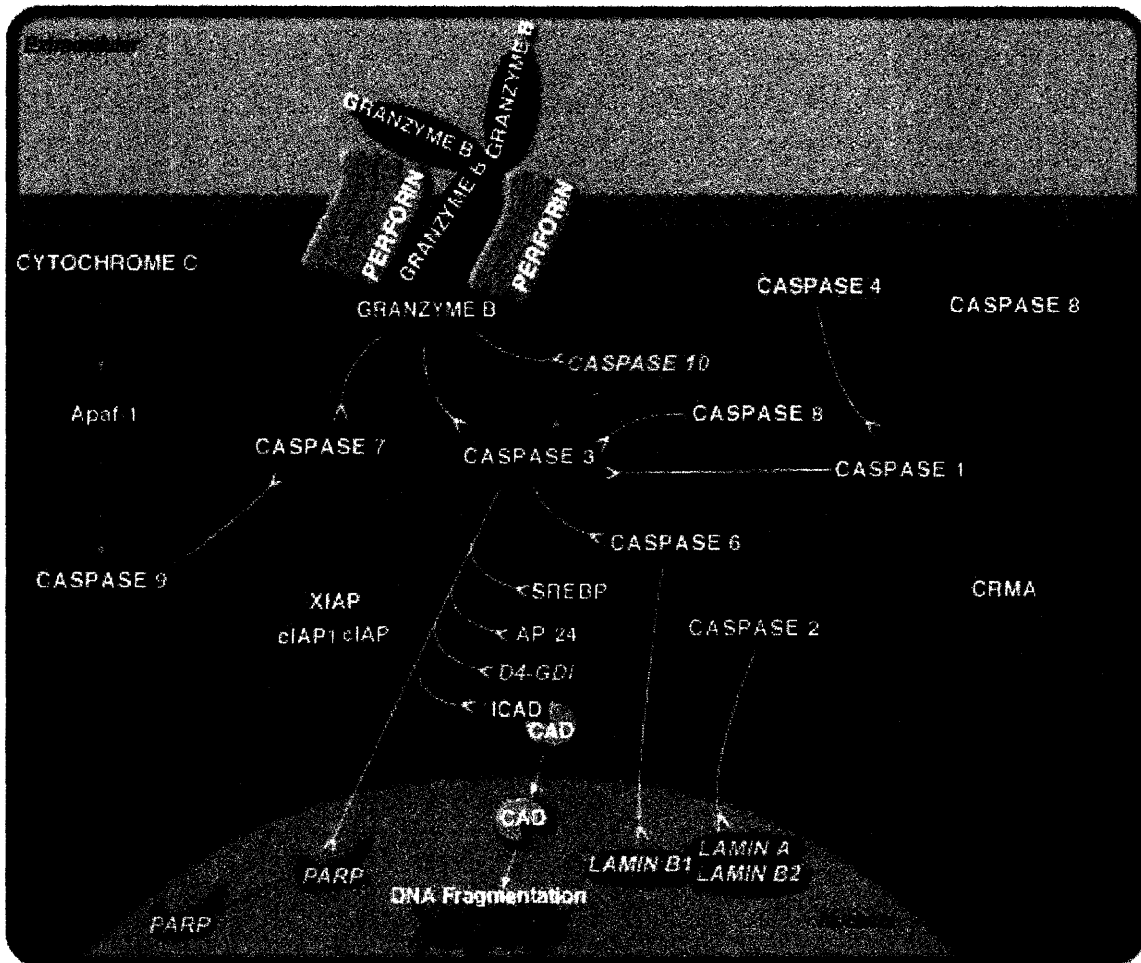
Figure 2. Caspase-dependent Apoptosis Pathway

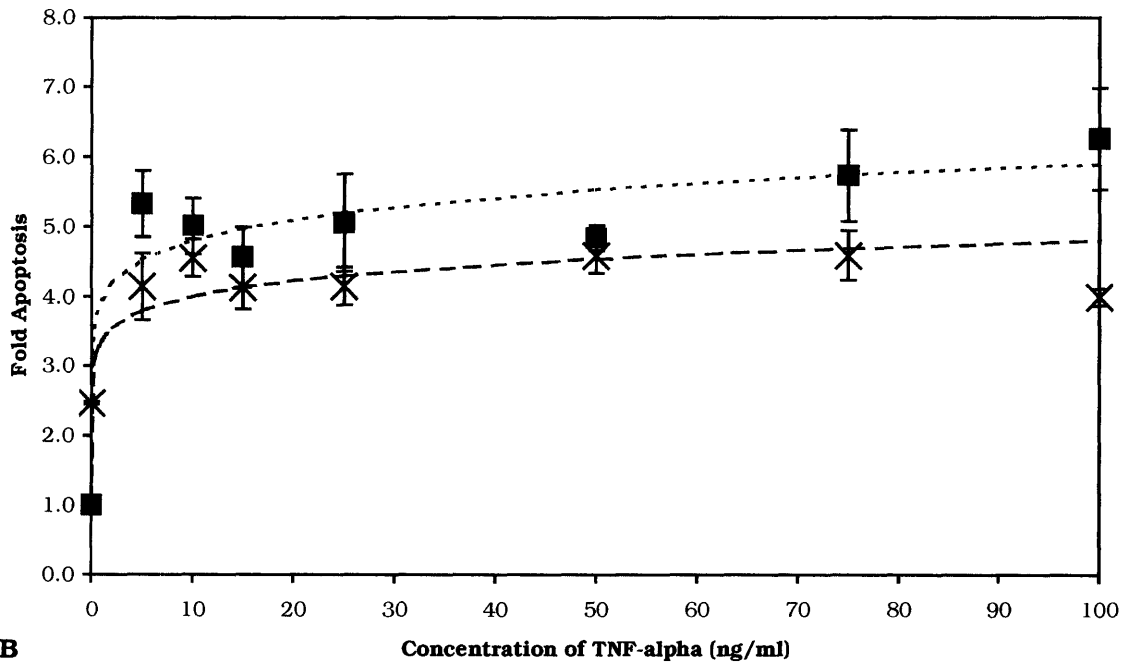Figure 3. Possible Signal Cascade of Nitric Oxide-induced Caspase Activation

Figure 4. Akt Signalling Pathway

49
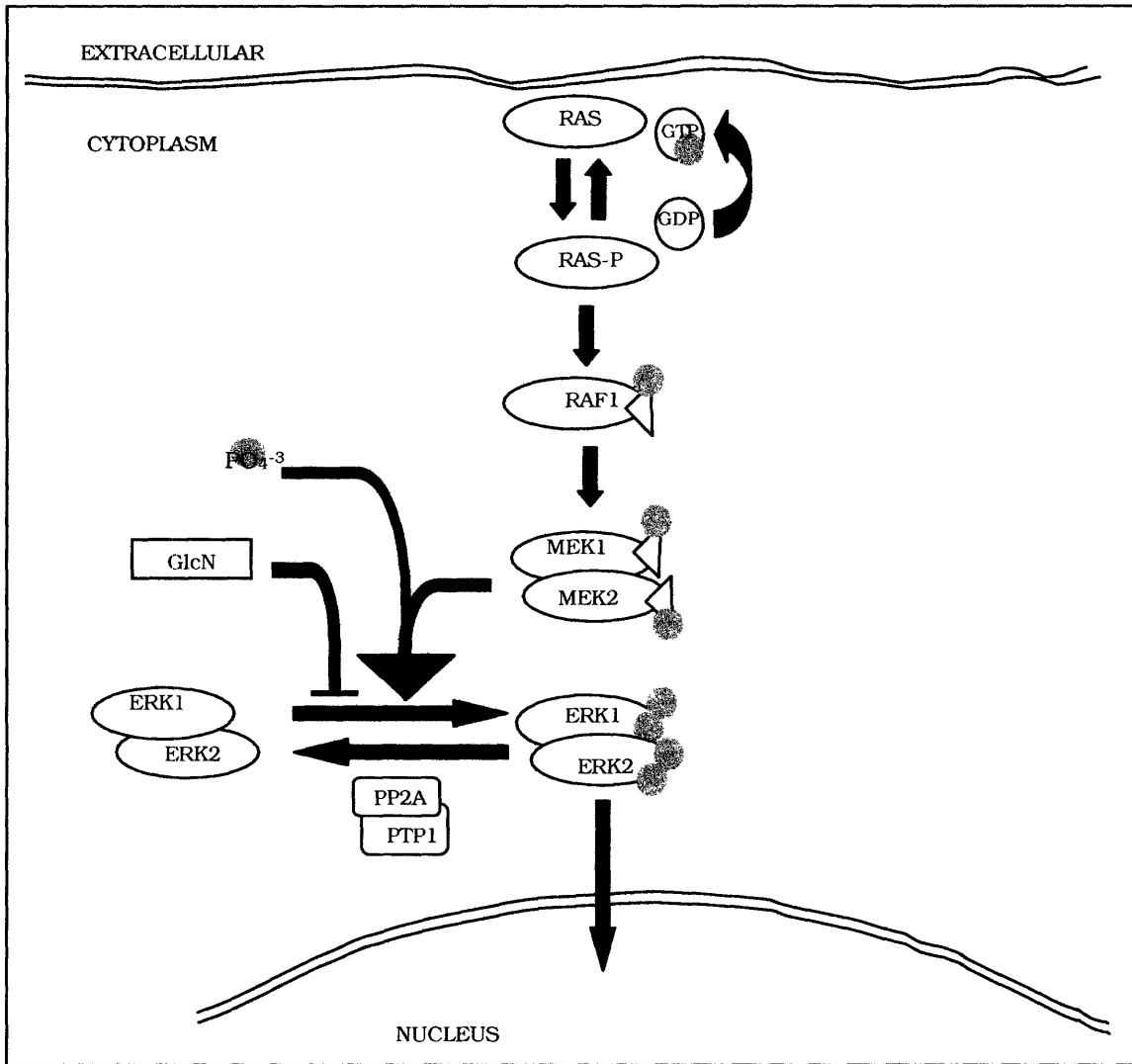
Figure 5. Possible MAPK Pathway with Glucosamine
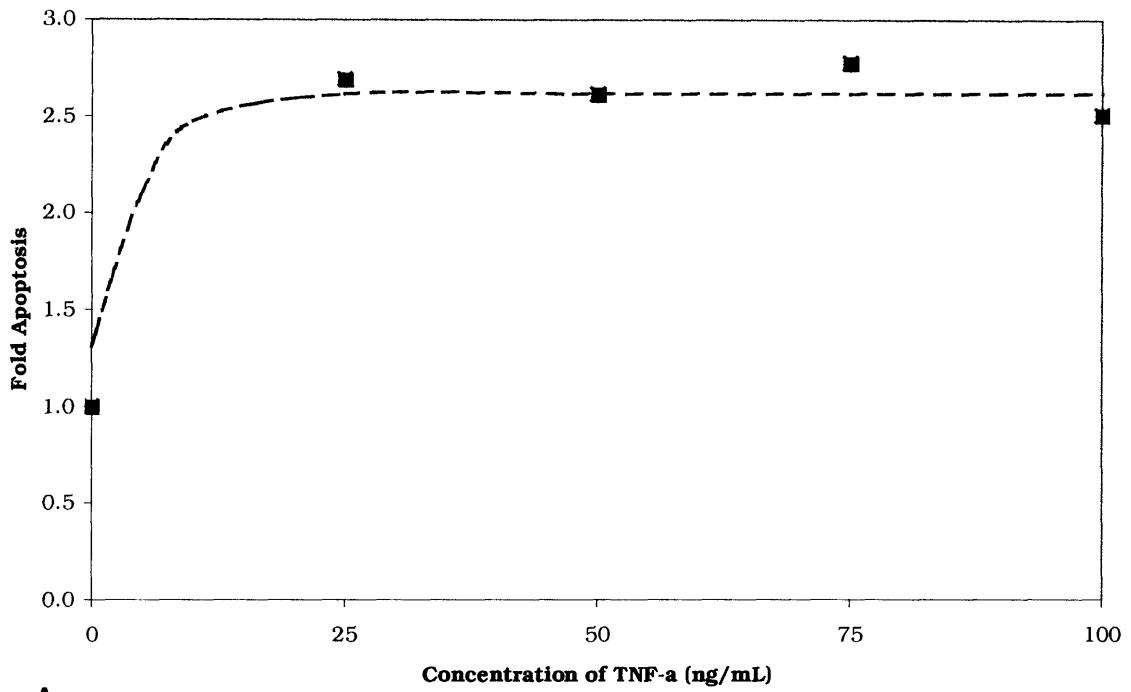
Figure 6. Dose Response for TNF-alpha in Cancer Cells.

Various concentrations of the death-inducing agent are added to (A) LNCaP cells and (B) HCT-116 cells and the relative amount of apoptosis is measured after 24 hours. In HCT-116 cells, 24-hour pre-treatment of 200 U/ml IFN-γ (--■--) is investigated, and compared with no pre-treatment (—✖—). In addition, the data are fit to sigmoid equations that best represent the dose response. (Refer the text for equations.)
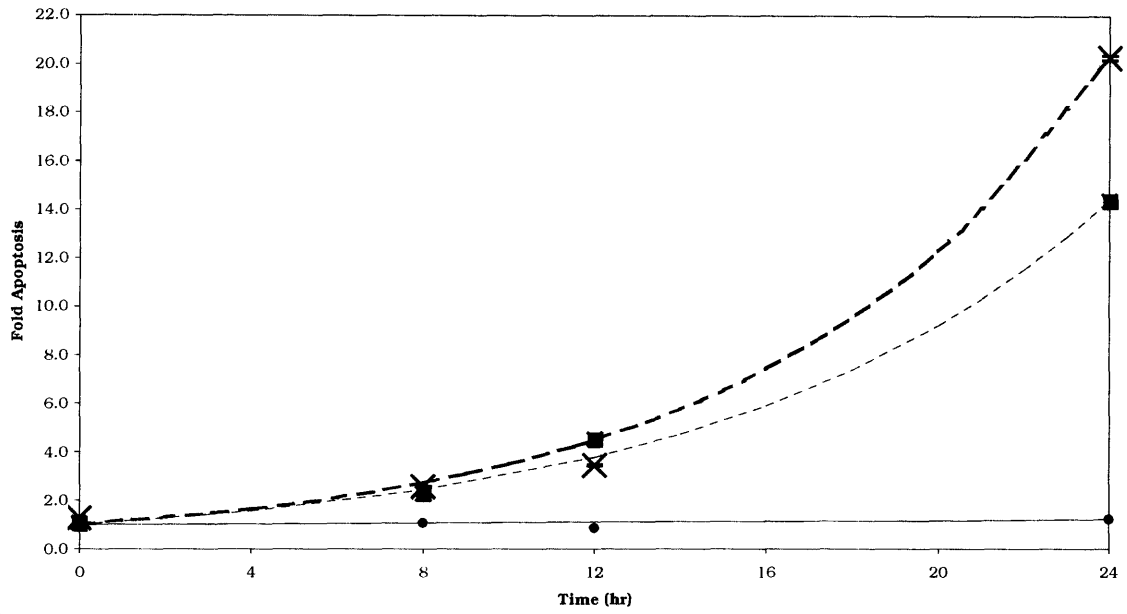
A
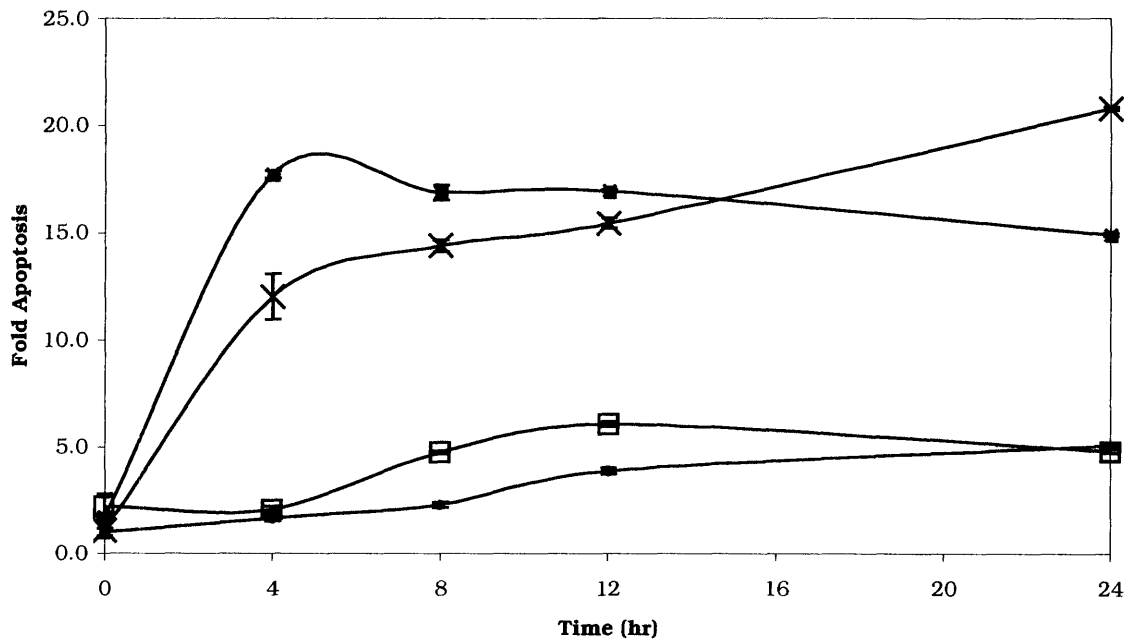
B
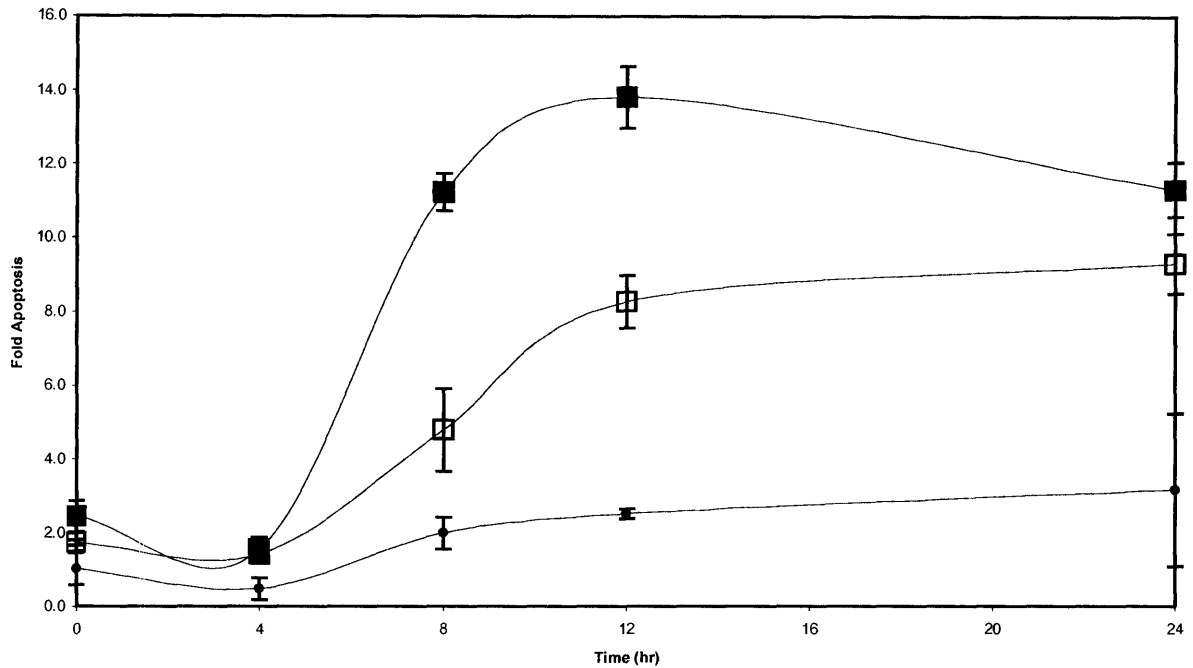
Figure 7. Cells' Response to TNF-alpha Over 24-hour Period
(A) LNCaP cells; untreated (•), treated with 50 ng/ml TNF-α (✕), and pre-treated for 24 hours with 200U/ml IFN-γ and then with 50 ng/ml TNF-α (■) show a slow response to the cytokine-induced apoptosis over the 24-hour period. (B) HCT-116 cells and (C) HT-29 cells, untreated (•), treated with TNF-α only (✕), IFN-γ only (□) and with TNF-α + IFN-γ (■) have a faster, more pronounced response than LNCaP cells.

54
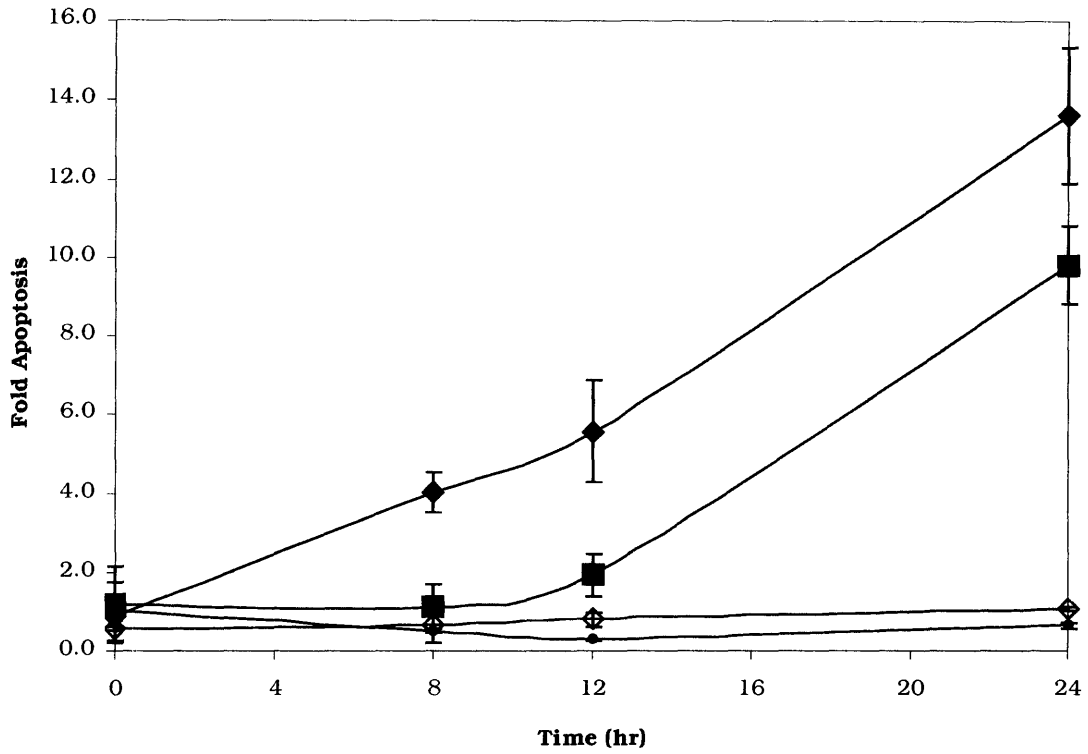
A
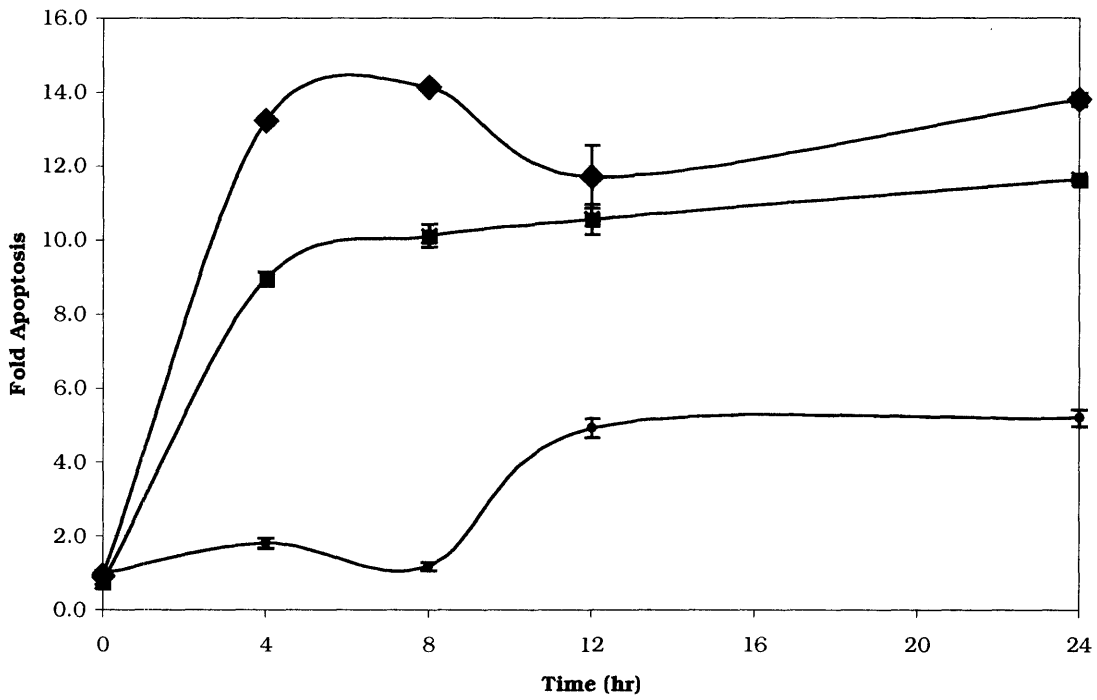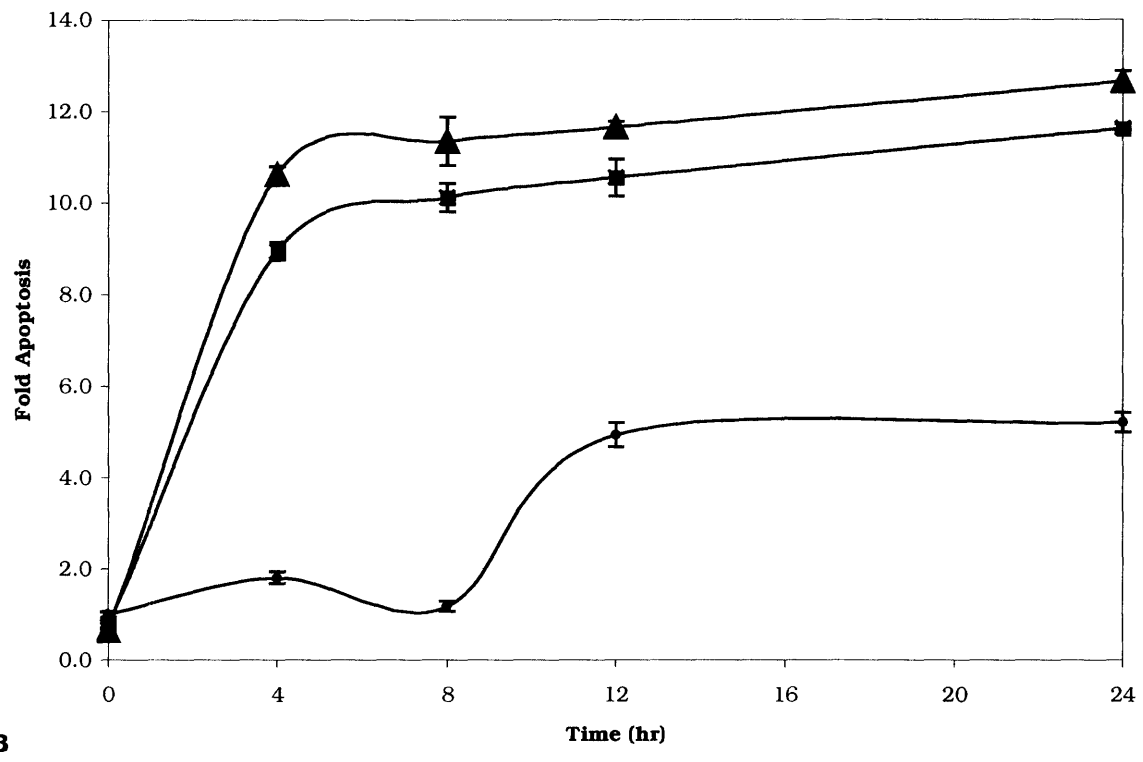

B

Figure 8. Effects of N-Methylarginine on TNF alpha-induced Apoptosis

Both (A) LNCaP and (B) HCT-116 cells show a reduction in apoptosis in response to 5 mM NMA (♦) in a background of 200 U/ml IFN-γ and 50 ng/ml TNF-α (■). Note that this nitric oxide synthase inhibitor is added concurrently with the cytokines. Control cells (•) have little or no response.

A

B
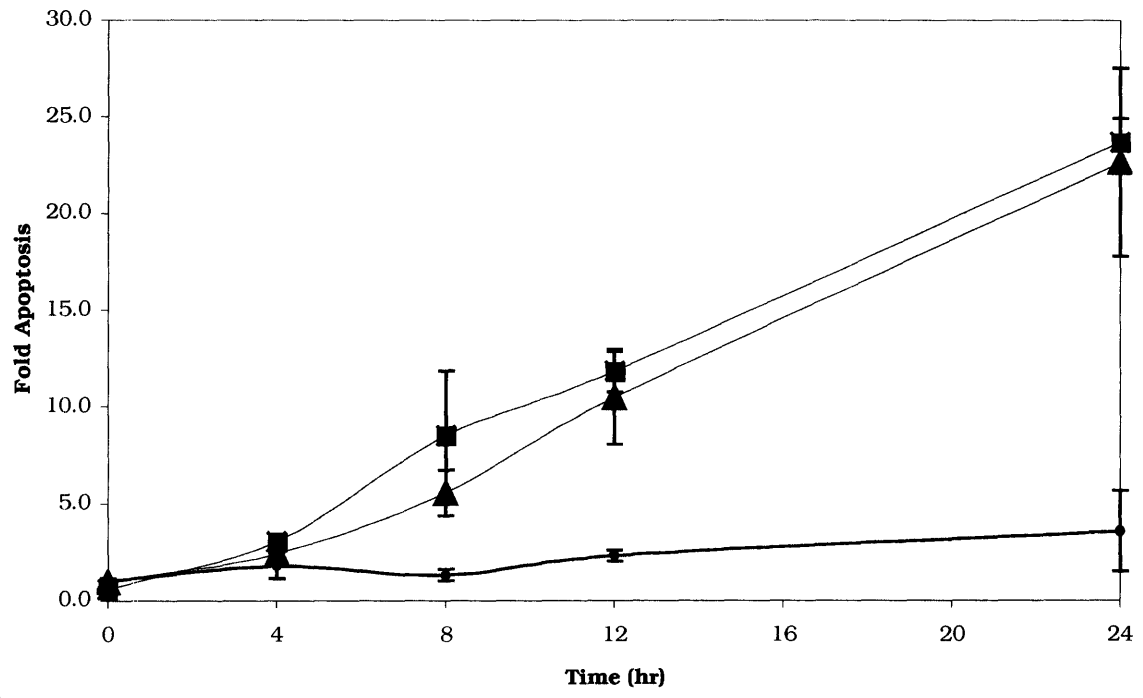
Figure 9. Effects of 1400W on TNF alpha-induced Apoptosis

57

The cancer cells are untreated (•) or induced into cell death with 200 U/ml IFN-γ and 50 ng/ml TNF-α. To the treated cells, is added also an iNOS inhibitor, 1400W, in a final concentration of 20 μM (▲). This infusion has little effect on both cancer cells, (A) LNCaP cells and (B) HCT-116 cells.

Table 2. Optical Density Measurements of Plasmid DNA

Sample Name	260/230	260/280	Concentration (µg/µl)
ARK5	2.03	1.88	1.830
ARK5 AS	2.09	1.90	1.702
ARK5 DN	2.11	1.89	1.712
GFP	2.24	1.87	3.953
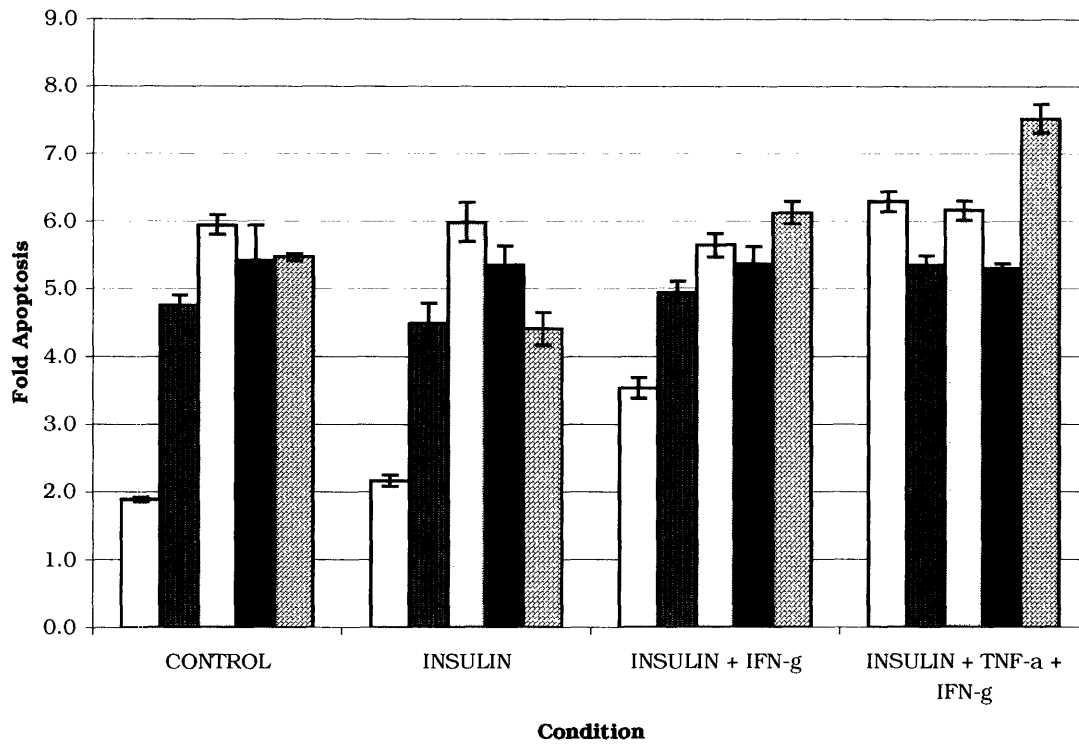
Figure 10. ARK5 Transfection into HT-29 cells

The bar graph compares with the control cells ( ), cells transfected with ARK5 (▧), ARK5 AS (▦), ARK5 DN (■) and GFP (▨) DNA into the cells using Invitrogen's Lipofectamine 2000. The plasmids are incubated for four hours before the OptiMEM is replaced with HT-29 growth medium. The cells were then pre-treated with 200 U/ml IFN-γ for 24 hours before the addition of 200 nM insulin and 50 ng/ml TNF-α. Fold apoptosis was then measured and calculated. There is no significant ARK5-specific effect on these cells although the transfection process itself induced much apoptosis.

A

B

61
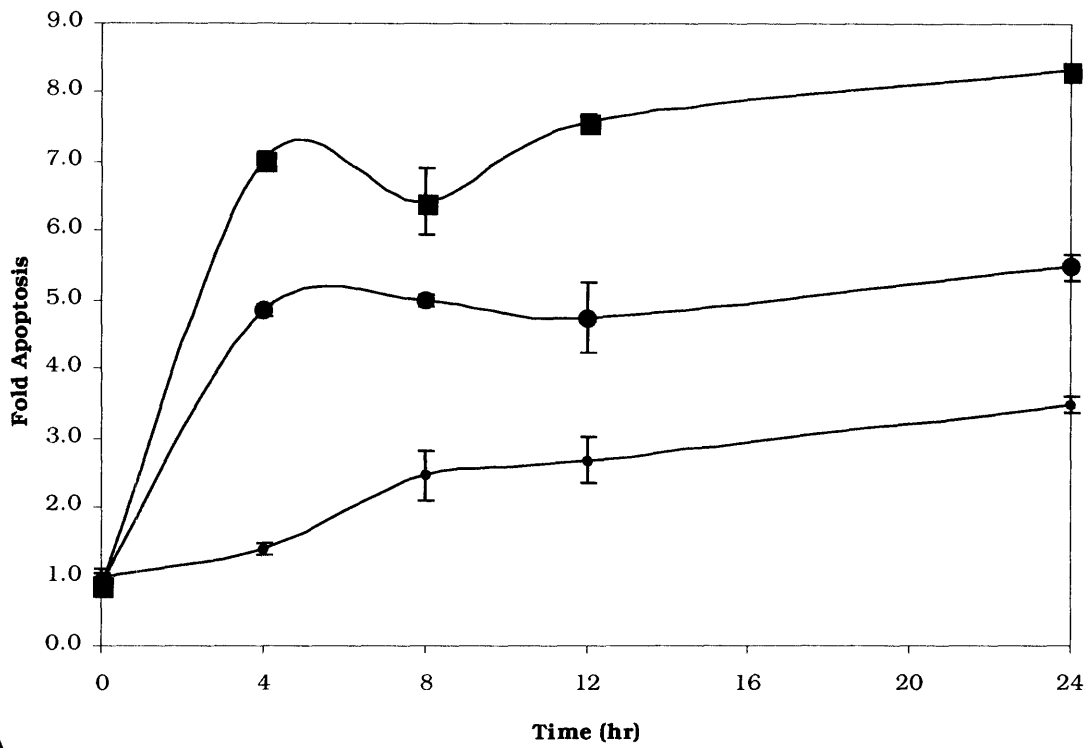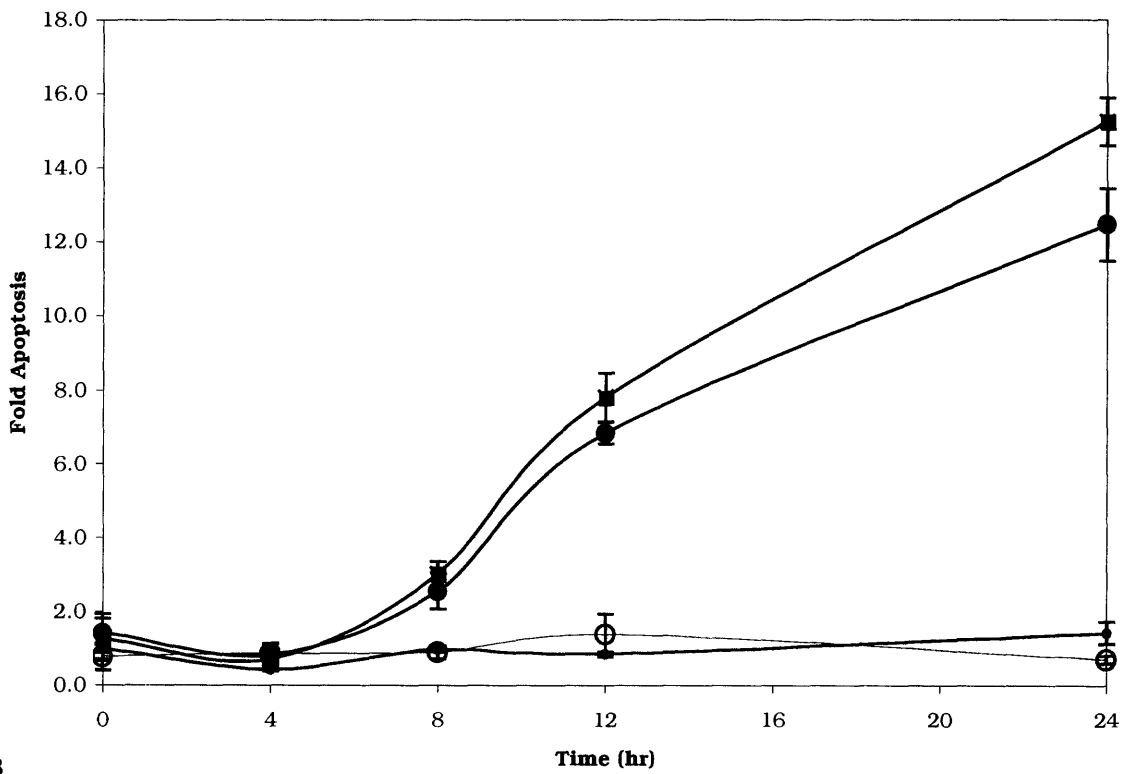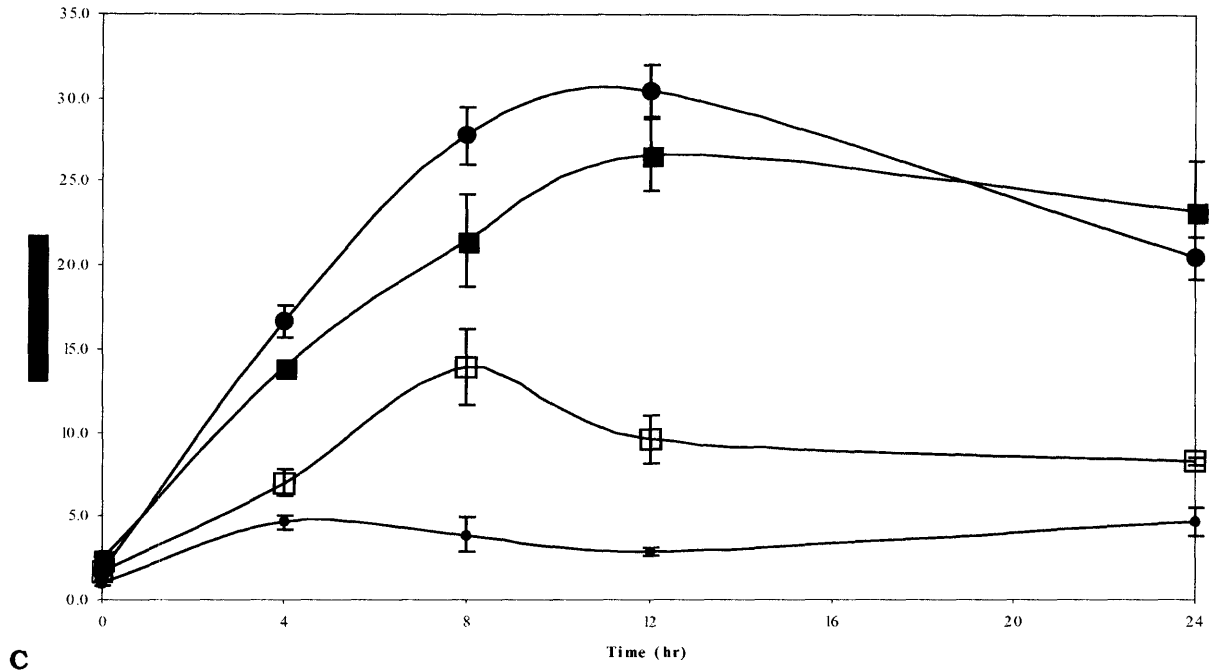
Figure 11. Effects of Glucosamine on TNF-alpha-induced Apoptosis

Four conditions are represented in these graphs, representing (A) HCT-116, (B) LNCaP and (C) HT-29 cells. Control cells (•) have no cytokines added. Twenty-four hours prior to harvesting, cells are treated with IFN-γ in conjunction with 50 ng/ml TNF-α (■) or, in the case of HT-29 cells, with only 200 U/ml IFN-γ (□). To the former is added, at the same time as TNF-α, 2 mM glucosamine (◆). After 24 hours, fold apoptosis is measured and calculated. The response from the three cell types does not clearly define the effects of glucosamine.
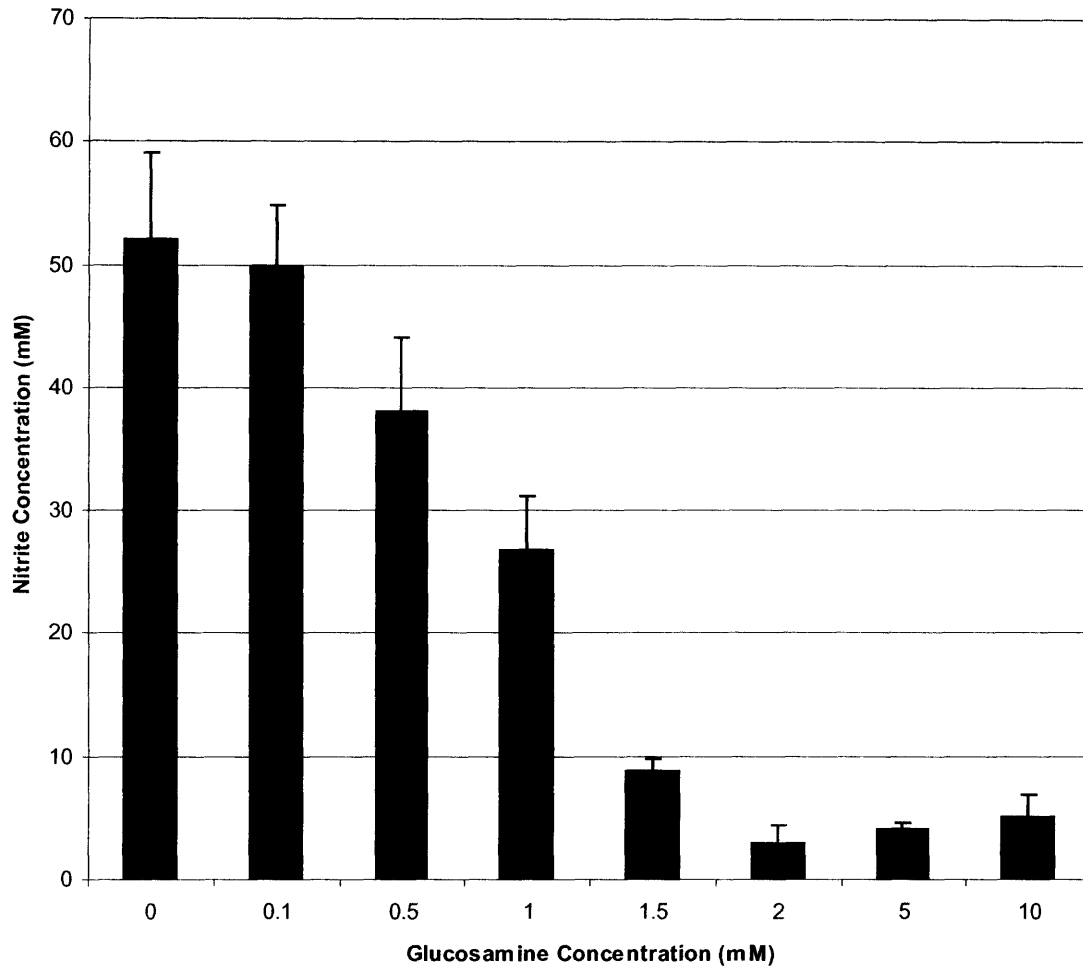
Figure 12. Dose Response of Glucosamine in RAW 264.7 Macrophages

The macrophages were plated two million cells per well and stimulated with 100 ng/ml LPS, 50 U/ml IFN-γ and, simultaneously, varying concentrations of glucosamine. The cell culture medium was collected after eight hours and nitrite levels were measured using the Griess Reaction.

APPENDIX B. PROTOCOLS

B.1 Plasmid Maxiprep

Protocol: Plasmid or Cosmid DNA Purification Using QIAfilter Plasmid Midi and Maxi Kits

This protocol is designed for preparation of up to 100 µg of high- or low-copy plasmid or cosmid DNA using the QIAfilter Plasmid Midi Kit, or up to 500 µg using the QIAfilter Plasmid Maxi Kit. In this protocol, QIAfilter Cartridges are used instead of conventional centrifugation to clear bacterial lysates. For purification of double-stranded M13 replicative-form DNA, we recommend using the protocol in Appendix H on page 79.

Low-copy plasmids which have been amplified in the presence of chloramphenicol should be treated as high-copy plasmids when choosing the appropriate culture volume.

Maximum recommended culture volumes*

	QIAfilter Midi	QIAfilter Maxi
High-copy plasmids	25 ml	100 ml
Low-copy plasmids	50–100 ml	250 ml[†]

* For high-copy plasmids, expected yields are 75–100 µg for the QIAfilter Plasmid Midi Kit and 300–500 µg for the QIAfilter Plasmid Maxi Kit. For low-copy plasmids, expected yields are 20–100 µg for the QIAfilter Plasmid Midi Kit and 50–250 µg for the QIAfilter Plasmid Maxi Kit using these culture volumes.

† The maximum recommended culture volume applies to the capacity of the QIAfilter Maxi Cartridge. If higher yields of low-copy plasmids are desired, the lysates from two QIAfilter Maxi Cartridges can be loaded onto one QIAGEN-tip 500.

Important points before starting

■ New users are strongly advised to read Appendix C: General Considerations for Optimal Results provided on pages 63–73 before starting the procedure.

■ If working with low-copy vectors, it may be beneficial to increase the lysis buffer volumes in order to increase the efficiency of alkaline lysis, and thereby the DNA yield. In case additional Buffers P1, P2, and P3 are needed, their compositions are provided in Appendix D: Composition of Buffers, on page 74. Alternatively, the buffers may be purchased separately (see page 83).

■ **Optional**: Remove samples at the steps indicated with the symbol ⓘ in order to monitor the procedure on an analytical gel.

QIAfilter Plasmid Midi/Maxi

Things to do before starting

■ Add the provided RNase A solution to Buffer P1 before use. Use one vial of RNase A (spin down briefly before use) per bottle of Buffer P1, to give a final concentration of 100 µg/ml.

■ Check Buffer P2 for SDS precipitation due to low storage temperatures. If necessary, dissolve the SDS by warming to 37°C.

■ Pre-chill Buffer P3 to 4°C.

■ In contrast to the standard protocol, the lysate is not incubated on ice after addition of Buffer P3.

Procedure

1. **Pick a single colony from a freshly streaked selective plate and inoculate a starter culture of 2–5 ml LB medium containing the appropriate selective antibiotic. Incubate for ~8 h at 37°C with vigorous shaking (~300 rpm).**

   Use a tube or flask with a volume of at least 4 times the volume of the culture.

2. **Dilute the starter culture 1/500 to 1/1000 into selective LB medium. For high-copy plasmids inoculate 25 ml or 100 ml medium. For low-copy plasmids, inoculate 50–100 ml or 250 ml medium. Grow at 37°C for 12–16 h with vigorous shaking (~300 rpm).**

   Use a flask or vessel with a volume of at least 4 times the volume of the culture. The culture should reach a cell density of approximately 3–4 x 10⁹ cells per ml, which typically corresponds to a pellet wet weight of approximately 3 g/liter medium (see page 68).

3. **Harvest the bacterial cells by centrifugation at 6000 x g for 15 min at 4°C.**

   6000 x g corresponds to 6000 rpm in Sorvall GSA or GS3 or Beckman JA-10 rotors. Remove all traces of supernatant by inverting the open centrifuge tube until all medium has been drained.

   ☺ If you wish to stop the protocol and continue later, freeze the cell pellets at –20°C.

4. **Resuspend the bacterial pellet in 4 ml or 10 ml Buffer P1.**

   For efficient lysis it is important to use a vessel that is large enough to allow complete mixing of the lysis buffers. Ensure that RNase A has been added to Buffer P1. The bacteria should be resuspended completely by vortexing or pipetting up and down until no cell clumps remain.

5. **Add 4 ml or 10 ml Buffer P2, mix gently but thoroughly by inverting 4–6 times, and incubate at room temperature for 5 min.**

   Do not vortex, as this will result in shearing of genomic DNA. The lysate should appear viscous. Do not allow the lysis reaction to proceed for more than 5 min. After use, the bottle containing Buffer P2 should be closed immediately to avoid acidification from CO_2 in the air.

During the incubation prepare the QIAfilter Cartridge:

Screw the cap onto the outlet nozzle of the QIAfilter Midi or QIAfilter Maxi Cartridge. Place the QIAfilter Cartridge in a convenient tube.

6. Add 4 ml or 10 ml chilled Buffer P3 to the lysate, and mix immediately but gently by inverting 4–6 times. Proceed directly to step 7. Do not incubate the lysate on ice.

Precipitation is enhanced by using chilled Buffer P3. After addition of Buffer P3, a fluffy white precipitate containing genomic DNA, proteins, cell debris, and SDS becomes visible. The buffers must be mixed completely. If the mixture still appears viscous and brownish, more mixing is required to completely neutralize the solution. It is important to transfer the lysate into the QIAfilter Cartridge immediately in order to prevent later disruption of the precipitate layer.

7. Pour the lysate into the barrel of the QIAfilter Cartridge. Incubate at room temperature (15–25°C) for 10 min. Do not insert the plunger!

Important: This 10 min incubation at room temperature is essential for optimal performance of the QIAfilter Midi or QIAfilter Maxi Cartridge. Do not agitate the QIAfilter Cartridge during this time. A precipitate containing proteins, genomic DNA, and detergent will float and form a layer on top of the solution. This ensures convenient filtration without clogging. If, after the 10 min incubation, the precipitate has not floated to the top of the solution, carefully run a sterile pipet tip around the walls of the cartridge to dislodge it.

8. Equilibrate a QIAGEN-tip 100 or QIAGEN-tip 500 by applying 4 ml or 10 ml Buffer QBT and allow the column to empty by gravity flow.

Flow of buffer will begin automatically by reduction in surface tension due to the presence of detergent in the equilibration buffer. Allow the QIAGEN-tip to drain completely. QIAGEN-tips can be left unattended, since the flow of buffer will stop when the meniscus reaches the upper frit in the column.

9. Remove the cap from the QIAfilter Cartridge outlet nozzle. Gently insert the plunger into the QIAfilter Midi or QIAfilter Maxi Cartridge and filter the cell lysate into the previously equilibrated QIAGEN-tip.

Filter until all of the lysate has passed through the QIAfilter Cartridge, but do not apply extreme force. Approximately 10 ml and 25 ml of the lysate are generally recovered after filtration.

 ι· Remove a 240 µl or 120 µl sample of the filtered lysate and save for an analytical gel (sample 1) in order to determine whether growth and lysis conditions were optimal.

10. Allow the cleared lysate to enter the resin by gravity flow.

 ι·ͻ Remove a 240 µl or 120 µl sample of the flow-through and save for an analytical gel (sample 2) in order to determine the efficiency of DNA binding to the QIAGEN Resin.

11. **Wash the QIAGEN-tip with 2 x 10 ml or 2 x 30 ml Buffer QC.**

Allow Buffer QC to move through the QIAGEN-tip by gravity flow. The first wash is sufficient to remove all contaminants in the majority of plasmid preparations. The second wash is especially necessary when large culture volumes or bacterial strains producing large amounts of carbohydrates are used.

ɪ⸱ Remove a 400 μl or 240 μl sample of the combined wash fractions and save for an analytical gel (sample 3).

12. **Elute DNA with 5 ml or 15 ml Buffer QF.**

Collect the eluate in a 10 ml or 30 ml tube. Use of polycarbonate centrifuge tubes for collection is not recommended as polycarbonate is not resistant to the alcohol used in subsequent steps.

ɪ⸱ Remove a 100 μl or 60 μl sample of the eluate and save for an analytical gel (sample 4).

⊛ If you wish to stop the protocol and continue later, store the eluate at 4°C. Storage periods longer than overnight are not recommended.

13. **Precipitate DNA by adding 3.5 ml or 10.5 ml (0.7 volumes) room-temperature isopropanol to the eluted DNA. Mix and centrifuge immediately at ≥15,000 x g for 30 min at 4°C. Carefully decant the supernatant.**

All solutions should be at room temperature in order to minimize salt precipitation, although centrifugation is carried out at 4°C to prevent overheating of the sample. A centrifugal force of 15,000 x g corresponds to 9500 rpm in a Beckman JS-13 rotor and 11,000 rpm in a Sorvall SS-34 rotor. Alternatively, disposable conical-bottom centrifuge tubes can be used for centrifugation at 5000 x g for 60 min at 4°C. Isopropanol pellets have a glassy appearance and may be more difficult to see than the fluffy, salt-containing pellets that result from ethanol precipitation. Marking the outside of the tube before centrifugation allows the pellet to be more easily located. Isopropanol pellets are also more loosely attached to the side of the tube, and care should be taken when removing the supernatant.

14. **Wash DNA pellet with 2 ml or 5 ml of room-temperature 70% ethanol and centrifuge at ≥15,000 x g for 10 min. Carefully decant the supernatant without disturbing the pellet.**

Alternatively, disposable conical-bottom centrifuge tubes can be used for centrifugation at 5000 x g for 60 min at 4°C. The 70% ethanol removes precipitated salt and replaces isopropanol with the more volatile ethanol, making the DNA easier to redissolve.

15. **Air-dry the pellet for 5–10 min, and redissolve the DNA in a suitable volume of buffer (e.g., TE buffer, pH 8.0, or 10 mM Tris·Cl, pH 8.5).**

    Redissolve the DNA pellet by rinsing the walls to recover all the DNA, especially if glass tubes have been used. Pipetting the DNA up and down to promote resuspension may cause shearing and should be avoided. Overdrying the pellet will make the DNA difficult to redissolve. DNA dissolves best under alkaline conditions; it does not easily dissolve in acidic buffers.

Determination of yield

To determine the yield, DNA concentration should be determined by both UV spectrophotometry and quantitative analysis on an agarose gel.

Agarose gel analysis

We recommend removing and saving aliquots during the purification procedure (samples 1–4). If the plasmid DNA is of low yield or quality, the samples can be analyzed by agarose gel electrophoresis to determine at what stage of the purification procedure the problem occurred (see page 60).

QIAfilter Plasmid
Midi/Maxi

B.2 Transfection

Transfection Procedure (for DNA)

Use the following procedure to transfect mammalian cells in a 24-well format. For other formats, see **Scaling Up or Down Transfections**. All amounts and volumes are given on a per well basis.

1. **Adherent cells:** One day before transfection, plate $0.5\text{-}2 \times 10^5$ cells in 500 µl of growth medium without antibiotics so that cells will be 90-95% confluent at the time of transfection.

   Suspension cells: Just prior to preparing complexes, plate $4\text{-}8 \times 10^5$ cells in 500 µl of growth medium without antibiotics.

2. **For each transfection sample**, prepare complexes as follows:

   a. Dilute DNA in 50 µl of Opti-MEM® I Reduced Serum Medium without serum (or other medium without serum). Mix gently.

   b. Mix Lipofectamine™ 2000 gently before use, then dilute the appropriate amount in 50 µl of Opti-MEM® I Medium. Incubate for 5 minutes at room temperature. **Note:** Combine diluted Lipofectamine™ 2000 with diluted DNA within 30 minutes.

   c. After 5 minute incubation, combine the diluted DNA with diluted Lipofectamine™ 2000 (total volume = 100 µl). Mix gently and incubate for 20 minutes at room temperature (solution may appear cloudy). **Note:** Complexes are stable for 6 hours at room temperature.

3. Add the 100 µl of complexes to each well containing cells and medium. Mix gently by rocking the plate back and forth.

4. Incubate cells at 37°C in a CO_2 incubator for 18-48 hours prior to testing for transgene expression. It is not necessary to change the medium, but medium may be replaced after 4-6 hours.

5. **For stable cell lines:** Passage cells at a 1:10 (or higher dilution) into fresh growth medium 24 hours after transfection. Add selective medium (if desired) the following day.

   For suspension cells: 4 hours post-transfection, add PMA and/or PHA (if desired) to enhance CMV promoter activity and increase gene expression.

Scaling Up or Down Transfections

To transfect cells in different tissue culture formats, vary the amounts of Lipofectamine™ 2000, DNA, cells, and medium used in proportion to the relative surface area, as shown in the table. With automated, high-throughput systems, a complexing volume of 50 µl is recommended for transfections in 96-well plates. Note: You may perform rapid 96-well plate transfections by plating cells directly into the transfection mix. Prepare complexes in the plate and directly add cells at twice the cell density as in the basic protocol in a 100 µl volume. Cells will adhere as usual in the presence of complexes.

Culture vessel	Surf. area per well (cm²)	Relative surf. area vs. 24-well	Vol. of plating medium	DNA (µg) in media vol. (µl)	Lipofectamine™ 2000 (µl) in media vol. (µl)
96-well	0.3	0.2	100 µl	0.2 µg in 25 µl	0.5 µl in 25 µl
24-well	2	1	500 µl	0.8 µg in 50 µl	2.0 µl in 50 µl
12-well	4	2	1 ml	1.6 µg in 100 µl	4.0 µl in 100 µl
35-mm	10	5	2 ml	4.0 µg in 250 µl	10 µl in 250 µl
6-well	10	5	2 ml	4.0 µg in 250 µl	10 µl in 250 µl
60-mm	20	10	5 ml	8.0 µg in 0.5 ml	20 µl in 0.5 ml
10-cm	60	30	15 ml	24 µg in 1.5 ml	60 µl in 1.5 ml

Note: Surface areas are determined from actual measurements of tissue culture vessels, and may vary depending on the manufacturer.

Optimizing Transfection

To obtain the highest transfection efficiency and low non-specific effects, optimize transfection conditions by varying cell density as well as DNA and Lipofectamine™ 2000 concentrations. Make sure that cells are greater than 90% confluent and vary DNA (µg):Lipofectamine™ 2000 (µl) ratios from 1:0.5 to 1:5.

B.3 Cell Death Detection ELISA

3.2   Preparation of working solutions

Reconstitution of lyophilizates   We strongly recommend double distilled water for reconstitution of lyophilisates :

Bottle #	Content	Reconstitution or preparation of working solution	Storage and stability	Use
1	Anti-histone-biotin	Reconstitute the lyophilizate in 450 µl double dist. water for 10 min and mix thoroughly.	at 2–8°C for 2 months	Part of the Immunoreagent
2	Anti-DNA-POD	Reconstitute the lyophilizate in 450 µl double dist. water for 10 min and mix thoroughly.	at 2–8°C for 2 months	Part of the Immunoreagent
3	Positive control	Reconstitute the lyophilizate in 450 µl double dist. water for 10 min and mix thoroughly.	at 2–8°C for 2 months	ELISA step 1

Preparation of kit working solutions   Please refer to the following table for the preparation of the ABTS solution

Reagent/ solution	Composition/preparation	Storage and stability	Use
ABTS tablets	Dependent on the number of samples tested, dissolve 1, 2, or 3 tablets from bottle 7 in 5, 10, or 15 ml Substrate Buffer (vial 6). Store protect from light! Allow to come to 15–25°C before use.	1 month, protect from light	ELISA step 5

7

3.2 Preparation of working solutions, continued

Preparation of the Immunoreagent

The Immunoreagent is prepared by mixing of 1/20 volume Anti-DNA-POD (bottle 2) and 1/20 volume Anti-histone-biotin (bottle 1) with 18/20 volumes Incubation buffer (bottle 4).

The following table shows the amounts needed for 10, 20, 40, 50, and 100 tests, respectively.
Note: Always prepare the solution shortly before use, do not store.

Step	Action
1	Place into a suitable vessel the Incubation buffer (bottle 4). Use the following table for the amount which is needed: | # of tests	10	20	40	50	100
---	---	---	---	---	---
Incubation buffer	720 µl	1440 µl	2880 µl	3600 µl	7200 µl	
2	• Add appropriate volumes of Anti-histone-biotin and Anti-DNA-POD. | # of tests	10	20	40	50	100
---	---	---	---	---	---
Anti-histone-biotin (bottle 1)	40 µl	80 µl	160 µl	200 µl	400 µl
Anti-DNA-POD (bottle 2)	40 µl	80 µl	160 µl	200 µl	400 µl
Immunoreagent total amount	800 µl	1600 µl	3200 µl	4000 µl	8000 µl	 • Homogenize thoroughly. *Note:* Do not store the solution. The solution is used in the ELISA Assay in step 2.

8

Roche Applied Science

3.3 Sample preparation

Before you begin The following cellular model system, in particular the cell number per test, is an example for a test procedure and is optimized therefore.

As a model system, the human lymphoma cell line U937 (ATCC CRL 1593) and the topoisomerase I-inhibitor camptothecin (22) was chosen for induction of apoptosis.

Cellular Assay Dilute the cells with culture medium to obtain a suitable cell concentration. Depending on the cell type and the cell death inducing agent, the cell number per test has to be determined and optimized. For adherent cells we recommend to trypsinize and wash the cells, seed amounts of cells in the MP wells (e.g. 10^4 or less) and let them grow for an appropriate while before starting the assay.

In the following table the procedure for a cellular assay is described:

Step	Action
1	Set up a titration of camptothecin (CAM) in declining concentrations from 4 μg/ml to 2 ng/ml. Duplicates of 100 μl/well are recommended. *Note:* Use cell culture medium without CAM as negative control.
2	Dilute exponentially growing U937 cells with culture medium to a concentration of 1×10^5 cells/ml.
3	Add 100 μl of diluted cells (10^4 cells) to each well.
4	Incubate for 4 hours at $37°$ C and 5% CO_2.
5	Centrifuge the MP 10 min. with 200 × g.
6	<table><tr><th>IF...</th><th>THEN...</th></tr><tr><td>you want to analyze necrosis</td><td>remove the supernatant carefully, and store it at $2-8°$ C.</td></tr><tr><td>you don't want to analyze the necrosis</td><td>remove the supernatant carefully.</td></tr></table>
7	• Resuspend the cell pellet in 200 μl Lysis buffer (bottle 5). • Incubate for 30 min at 15–25°C (Cell lysis). *Note:* Adherent cells can be lysed directly in the well without prior removal.
8	• Centrifuge the lysate at 200 × g for 10 min. • Transfer 20 μl from the supernatant (=cytoplasmic fraction) carefully into the streptavidin coated MP for analysis. Do not shake the pellet (cell nuclei, containing high molecular weight, unfragmented DNA). *Note:* Samples should be analyzed **immediately,** because storage at 2–8°C or −15 to −25°C reduces the ELISA signals.

Roche Applied Science

3.4   ELISA Assay

Before you begin   The ELISA was developed and evaluated with the use of 20 µl sample and 80 µl Immunoreagent per MP-well. It is recommended not to change these portions.

Cell equivalent   Using 10^4 cells/well (200 µl), the sample analyzed (20 µl lysate or supernatant) corresponds to a cell equivalent of 1×10^3 cells/well or 5×10^4 cells/ml.

Procedure   Please refer to the following table to perform the ELISA.

Note: It is recommended to analyze at least duplicates of the samples. Also, a negative control (cells without CAM treatment) should be analyzed, which allows calculation of an enrichment factor. Working temperature 18–25°C.

Step	Action
1	Transfer 20 µl from • culture supernatants after centrifugation and treatment (CAM) • lysates of CAM treated cells after centrifugation • positive control (bottle 3) • negative control (culture supernatant and lysate after centrifugation of untreated cells) • background control (Incubation buffer, bottle 4) into the MP. *Note:* It is important, due to low volumes, to pipette into the middle of the microplate well.
2	Add to each well 80 µl of the **Immunoreagent**.
3	Cover the MP with an adhesive cover foil. Incubate on a MP shaker under gently shaking (300 rpm) for 2 h at 15–25°C.
4	• Remove the solution thoroughly by tapping or suction. • Rinse each well 3 × with 250–300 µl **Incubation buffer** (bottle 4). • Remove solution carefully.
5	• Pipette to each well 100 µl **ABTS solution**. • Incubate on a plate shaker at 250 rpm until the color development is sufficient for a photometric analysis (approx. after 10–20 min.)
6	Measure at 405 nm against ABTS solution as a blank (reference wavelength approx. 490 nm).

Roche Applied Science